INTRACORTICAL MYELIN IN BIPOLAR DISORDER TYPE I AND THE IMPACTS OF NEUREGULIN-1 VARIATION AND AGE

INTRACORTICAL MYELIN IN BIPOLAR DISORDER TYPE I AND THE IMPACTS OF NEUREGULIN-1 VARIATION AND AGE

Katrina N. Kidd
H.B.Sc.

A thesis submitted to the School of Graduate Studies in partial fulfilment of the requirements for the degree Master of Science

McMaster University

MASTER OF SCIENCE (2023)

MCMASTER UNIVERSITY

Hamilton, Ontario

DEPARTMENT: Neuroscience

TITLE: Intracortical myelin in bipolar disorder type I and the impacts of neuregulin-1 variation and age

AUTHOR: Katrina N. Kidd, H.B.Sc.

SUPERVISOR: Dr. Benicio N. Frey, M.D., M.Sc., Ph.D.

COMMITTEE MEMBERS: Dr. Nicholas Bock, Ph.D., Dr. Luciano Minuzzi, M.D., Ph.D.

NUMBER OF PAGES: xv, 120

Lay Abstract

Bipolar disorder is associated with neurobiological changes, including cortical abnormalities, contributing to a greater disorder burden. Cortical myelination changes throughout the lifetime and larger deficits are found in individuals with bipolar disorder. However, the role of genetics in these intracortical myelin deficits is largely unknown. This thesis investigates how intracortical myelin content in various regions of the cortex is impacted by age, bipolar disorder diagnosis, and neuregulin gene variants. The goal of this research is to contribute to a better understanding of how genetics and age impact intracortical myelin in bipolar disorder to better understand the neurobiological changes of the disorder.

Abstract

Introduction: Bipolar disorder is associated with cortical abnormalities, including deficits in intracortical myelination. Intracortical myelin follows an inverted-U trajectory over the lifetime, but this trajectory is blunted in individuals with bipolar disorder. Little is understood about which genetic factors contribute to these deficits. Neuregulin-1, a cell-signalling protein, has been shown to contribute to cortical abnormalities and increase susceptibility to related disorders. Assessing the prevalence of neuregulin-1 polymorphisms, notably rs6994992, in bipolar disorder may elucidate the genetic contributors of intracortical myelin deficits and increase our understanding of factors causing susceptibility to bipolar disorder.

Methods: 67 participants with bipolar disorder type I and 75 healthy control participants were included. T_1-weighted MRI images were collected and processed to create R_1 cortical maps, a proxy measure of intracortical myelin. Participant blood samples were genotyped at the rs6994992 locus. Linear models were used to test whether intracortical myelin can be predicted by age, bipolar diagnosis and *NRG1* genotype.

Results: Intracortical myelin is significantly predicted by age, diagnosis and genotype together in the motor cortex (left: $R^2 = 0.09$, $p < 0.01$, right: $R^2 = 0.06$, $p < 0.05$), the right premotor cortex ($R^2 = 0.095$, $p < 0.001$), and the right inferior frontal cortex ($R^2 = 0.098$, $p < 0.001$). Age is a significant individual predictor of intracortical myelin in the right dorsal anterior cingulate cortex, the bilateral motor cortex, the right premotor cortex, and the right inferior frontal cortex.

Conclusions and Future Directions: Our study suggests that the right premotor, bilateral primary motor, and right inferior frontal cortices are regions of interest for understanding how intracortical myelin changes throughout the lifetime, especially in bipolar disorder. Future work should examine the impact of polygenic risk scores of bipolar disorder on intracortical myelin.

Acknowledgements

I would like to thank every person who supported me throughout the course of my degree and who helped with the completion of this project. First and foremost, I would like to express my immense gratitude to my supervisor, Dr. Benicio Frey, for his constant guidance and reassurance throughout my degree. I am grateful for his encouragement to find a project that I was passionate about and for allowing me to craft each aspect of this analysis. The experiences that I have had under his supervision and the knowledge I have gained have shaped me as a researcher, and I will carry them with me in all of my future endeavours.

I would like to thank my committee members, Dr. Nicholas Bock and Dr. Luciano Minuzzi, for acting as additional mentors and secondary supervisors to me. I am grateful for their contributions to my project's completion and for their support in ensuring I put forth my best work. I appreciate all of the discussions we had that taught me valuable lessons and were integral to my project.

I would like to thank the BioMac lab and each person I met during my time as a master's student. I am grateful for the sense of community I felt from each member of the lab and the support I received for each accomplishment, no matter how small. Particularly, I would like to thank the members of the Centre for Clinical Neurosciences, with whom I spent countless hours. I want to thank Dr. Bianca Wollenhaupt de Aguiar for her help with the genetic component of this project; it would not have been possible without her expertise. I would like to express my gratitude for how she professionally and personally supported me over the past two years. I want to thank Niousha Gazor and Mohammad Ali for every pipette tip discarded, every question answered, and every minute spent extracting DNA together. I could not have asked for two more inspiring individuals to have made as friends these past two years.

I would like to express my love and gratitude towards my family and friends, who always encouraged me to persist in the face of difficulty and listened to me ramble endlessly about this project. I am forever grateful for the kindness and compassion you all have shown me. A special thanks to Matthew for showing me that the journey is more important than the destination.

Finally, I would like to thank McMaster University and the Neuroscience Graduate program for teaching me valuable skills and for making my master's degree an experience I will take with me in the future. Thank you.

Table of Contents

List of Figures

List of Tables

List of Abbreviations and Symbols

Anterior cingulate cortex	ACC
Anterior insular cortex	AIC
Analysis of variance	ANOVA
Brain extraction tool	BET
Dorsal anterior cingulate cortex	dACC
Central nervous system	CNS
Epidermal growth factor	EGF
Echo-planar images	EPI
Functioning Assessment Short Test	FAST
Fronto-insular cortex	FIC
General Electric	GE
Genome-wide association study	GWAS
Intracortical myelin	ICM
Inferior frontal cortex	IFC
Inversion ratio	IR
Look Up Table	LUT
Montgomery-Asberg Depression Rating Scale	MADRS
Magnetic resonance	MR
Magnetic resonance imaging	MRI
N-methyl-D-aspartic acid	NMDA
Neuregulin 1	NRG1
Oligodendrocyte progenitor cell	OPC
Polymerase chain reaction	PCR
Proton density	PD
Proton density-weighted	PDW
Post-traumatic stress disorder	PTSD
Longitudinal relaxation rate	R_1
Region of interest	ROI
Real-time polymerase chain reaction	RT-PCR
Structured Clinical Interview for the DSM-V	SCID-5
Single nucleotide polymorphism	SNP
T_1-weighted	T_1w
T_2-weighted	T_2w
Young Mania Rating Scale	YMRS

Declaration of Academic Achievement

This thesis comprises 5 chapters: Chapter 1 is an introduction to the primary topics of study, including bipolar disorder, intracortical myelin, neuregulin-1, and the salience network. This section also includes an introduction to the aims and hypotheses of the study. Chapter 2 provides a detailed outline of the methods used in this study. Chapter 3 summarized all of the results from the analyses performed. Chapter 4 is a discussion section summarizing key findings, past research that relates to the current experiment, thoughts on future research and conclusions. Finally, chapter 5 includes references for all sources used in this thesis.

The data used in this experiment are part of a larger longitudinal study conducted at multiple sites at institutions across Canada and centred at McMaster University. The collection of all samples took place from 2017 to 2022. The study was conceived and designed by Dr. Benicio Frey, Dr. Nicholas Bock, Dr. Luciano Minuzzi, Dr. Flavio Kapczinski and co-investigators across the various research sites prior to my starting as a graduate student. Processing of intracortical myelin took place from 2021 to 2023 and was led by Dr. Nicholas Bock. Processing of blood samples took place from 2021 to 2022 and was completed by myself, Niousha Gazor and Mohammad Ali. Genotyping took place in 2023 and was completed by myself and Niousha Gazor. Statistical analyses were performed by myself with the help of Dr. Luciano Minuzzi and Dr. Nicholas Bock. The contents of this thesis were written by myself, except for the magnetic resonance imaging methods section (Section 2.5), which was completed with the assistance of Dr. Nicholas Bock and Stella Heo.

CHAPTER 1 - INTRODUCTION

1.1 Bipolar Disorder

1.1.1 Introduction to bipolar disorder

Bipolar disorder is a neuropsychiatric disorder with severe adverse clinical and functional outcomes characterized by periods of disturbed mood ranging from severe mania to depression (American Psychiatric Association, 2013). Bipolar disorder is the 17th leading cause of disability worldwide (Vigo et al., 2016), with a lifetime prevalence of 2.4% (Merikangas et al., 2011). Clinically, bipolar disorder is distinguished into three primary subtypes: bipolar disorder type I, bipolar disorder type II, and cyclothymic disorder. These distinctions are made depending on the type of mood episode an individual experiences. Bipolar disorder type I is characterized by manic episodes and possible depressive episodes. Bipolar disorder type II is characterized by depressive episodes and less severe manic episodes known as hypomanic episodes. Individuals with cyclothymia experience cyclical periods of mood disruptions that are less severe than other subtypes of bipolar disorder. It is also possible for individuals with bipolar disorder to experience mixed episodes in which they meet the criteria for a depressive episode and a manic episode simultaneously. According to DSM-5 criteria, individuals can meet the criteria for a mood episode if symptoms are present for one week for a manic episode and two weeks for a depressive episode (American Psychiatric Association, 2013).

When individuals with bipolar disorder are not in a current mood episode, they enter into a state of clinical remission known as euthymia, which may be associated with subsyndromal mood symptoms (American Psychiatric Association, 2013). However, despite not experiencing significant clinical symptoms, euthymic individuals experience neuropsychological and functional deficits that contribute to a lifelong burden of bipolar disorder. These impairments and residual symptoms are observed even after the remission of clinical mood episodes (Samalin et al., 2016). Often, individuals who experience clinical euthymia are unable to return to premorbid levels of functioning (Sanchez-Moreno et al., 2009). The average age of onset of bipolar disorder is 25 years, although onset during childhood has been observed and is often associated with a worsened prognosis (Baldessarini et al., 2010; Joslyn et al., 2016).

Bipolar disorder can be accompanied by comorbid psychiatric conditions, including anxiety, borderline personality disorder and attention deficit hyperactivity disorder (Frías et al., 2016; Nierenberg et al., 2005; Simon et al., 2004). Anxiety disorders are the most common comorbid disorder for individuals with bipolar disorder, with an estimated prevalence of 45% (Pavlova et al., 2015). These high rates of comorbidity can increase the burden of illness for individuals with bipolar disorder and contribute to difficulty in diagnosis and treatment. Another common comorbid feature of bipolar disorder is the presence of psychotic symptoms, such as hallucinations, which occur in an estimated 35-60% of manic episodes (Dunayevich & Keck, 2000). These symptoms in individuals with bipolar disorder contribute to deficits in psychosocial functioning and neurocognition and have been associated with cortical thinning, among other brain changes (Bora, 2018; Hibar et al., 2018; Levy et al., 2013). Together, comorbidities contribute to the burden of bipolar disorder throughout the lifetime and lead to a worsened illness prognosis.

1.1.2 The role of genetics in bipolar disorder

Bipolar disorder has been shown to have a high degree of genetic heritability that contributes to the risk of developing the disorder. Studies performed on monozygotic twins indicate that heritability is estimated at 70-90% (Smoller & Finn, 2003). A portion of this estimated heritability can be explained by single-nucleotide polymorphisms (SNPs), minor changes in an individual's genome. Results from genome-wide association studies (GWAS) assessing the genetic risk for bipolar disorder estimate that 25% of the heritability of bipolar disorder can be explained by the combined effect of common variants (Gordovez & McMahon, 2020; Stahl et al., 2019). In particular, SNPs have small effect sizes but interact with the environment to contribute to a large portion of the risk of developing bipolar disorder (Gordovez & McMahon, 2020). However, one recent GWAS highlights that only 8% of the heritability of bipolar disorder can be explained by SNPs that have already been identified and that larger sample sizes are necessary to determine additional SNPs involved in the risk of developing bipolar disorder (Stahl et al., 2019).

These genetic variants can alter the expression of various bipolar-associated genes, contributing to structural and functional neurobiological changes. For example, altered expression of myelin-related genes in the prefrontal cortex has been observed in bipolar disorder, along with a measurable decrease in the number of oligodendrocytes

(Kim & Webster, 2010; Savitz et al., 2014; Tkachev et al., 2003). Abnormal expression of myelin-associated genes contributes to altered connectivity between the prefrontal cortex and subcortical regions, further hindering functioning in bipolar disorder (Bellani et al., 2016; Tkachev et al., 2003).

1.1.3 Structural brain changes in bipolar disorder

The period of early to mid-adulthood is a time of psychological vulnerability when individuals, on average, are more likely to develop bipolar disorder (Baldessarini et al., 2010). During this time, the cerebral cortex is also undergoing important structural development, including the development of cortical myelin (Grydeland et al., 2013). The onset of bipolar disorder during this essential neurodevelopmental period can lead to deficits in the structure and function of the cortex (Gogtay et al., 2004). Within deep white matter tracts of the brain, bipolar disorder has been associated with altered integrity, density, and volume of white matter (Favre et al., 2019; Houenou et al., 2007; Sussmann et al., 2009). Grey matter alterations have also been observed in bipolar disorder studies, finding decreased volume in various regions of the cerebral cortex associated with bipolar disorder (Selvaraj et al., 2012; Wise et al., 2017).

These neurobiological abnormalities, located in areas related to bipolar disorder, have been associated with adverse outcomes of the disorder, including deficits in neurocognition and severity of symptoms (Nery et al., 2009; Poletti et al., 2015). The heritability of bipolar disorder extends to these white matter abnormalities, with some studies finding that white matter deficits are found in unaffected relatives of those with bipolar disorder (McDonald et al., 2004). However, the directionality of these relationships is yet to be elucidated. Some white matter abnormalities may convey susceptibility to developing the disorder, while others may result from the disorder, contributing to the lifetime illness burden (Hajek et al., 2005).

1.2 Intracortical Myelination

1.2.1 Functions of myelination

Myelin sheaths are a type of tissue found in the nervous systems that wrap around neuronal axons to insulate and increase conduction velocity through a process known as saltatory conduction (Morell & Quarles, 1999). Myelin primarily comprises lipids (70-85%) with a high cholesterol content, allowing the sheaths to form a barrier between the axon and surrounding interstitial fluid (O'Brien, 1965; Quarles et al., 2006). In the central nervous system (CNS), myelin sheaths are formed from oligodendrocytes, a type of glial cell that supports neurons. In the peripheral nervous system, these sheaths are made from different neuroglia known as Schwann cells (Morell & Quarles, 1999). In both systems, the individual cells wrap around neuronal axons to form an insulating barrier that speeds conduction velocity by increasing axon membrane thickness and limiting ion leakage (Haines, 2001; Ohvo-Rekilä et al., 2002).

In the CNS, myelin density is greatest in primary sensory and motor regions that require quick signalling (Sanides, 1969). In opposition, association areas for higher-order processes are the most lightly myelinated regions. In addition to regional variability, myelination in the brain is also depth-dependent. Findings from post-mortem studies indicate that deeper layers of the cortex (IV-VI) are the most heavily myelinated in comparison to shallow cortical regions (I-III), which are more lightly myelinated (Glasser & Van Essen, 2011). Deep white matter tracts in the brain are composed of large amounts of myelin, which allow them to send signals between brain regions quickly. However, myelin is also found in smaller amounts outside of these white matter tracts in grey matter and subcortical brain structures. In these regions, myelinated axons are less involved in quick signal transduction and instead play a role in other neural activities, including synaptic plasticity (Timmler & Simons, 2019). Through this role, myelination increases the capacity for learning and promotes memory recall (McKenzie et al., 2014; Pan et al., 2020).

Oligodendrocytes in the CNS are developed from oligodendrocyte progenitor cells (OPC) through a process of proliferation, migration, and differentiation to form mature myelin sheaths (Bradl & Lassmann, 2010). Essential proteins, including myelin basic protein, regulate myelin formation by oligodendrocytes. The degree of myelination, axon size and myelin thickness can be regulated by the expression of these proteins (Shine et al., 1992). Myelination is strictly coordinated by various genetic signalling cascades, particularly during fetal development and throughout the lifetime. Small mutations in these cascades can drastically affect signal transduction throughout the brain (Schmitt et al., 2020).

1.2.2 Intracortical myelination

Intracortical myelin (ICM) consists of myelinated fibres within the grey matter of the cerebral cortex that aid in neuronal metabolic support and synaptic plasticity (Micheva et al., 2016; Timmler & Simons, 2019). The thickness of the cerebral cortex reflects not only the density of neurons but also glial cell density, including oligodendrocytes (Zatorre et al., 2012). Cortical thickness is thus a measure of interest when studying myelin. As mentioned previously, myelin is regionally dependent in the cortex. ICM density is greatest in primary sensory and motor regions but lightest in association areas, such as the insula and cingulate cortex, indicating that myelin density is influenced by function (Nieuwenhuys, 2013). Once heavy myelination is established in motor and sensory regions, it remains resistant to change to perform basic human functions. Conversely, light myelination in association areas is necessary to allow these regions to change in response to experience (Glasser et al., 2014). In healthy individuals, our group has shown that there are no sex differences in ICM after taking into account differences in intracranial volume (Rowley et al., 2017).

Rather than playing a role in salutatory conduction, ICM alters signal transduction by synchronizing the conduction velocity of an entire neuronal network (Pajevic et al., 2014). ICM also benefits synaptic remodelling in the cortex by acting as a growth inhibitor. It does so by releasing myelin-associated inhibitors, which prevent the growth of harmful synaptic connections and impede the regeneration of neurons in an experience-dependent manner (Filbin, 2003; McGee et al., 2005). This is proposed to be beneficial in lightly myelinated grey matter regions of the cortex to improve efficiencies of synaptic remodelling (Timmler & Simons, 2019).

1.2.3 Intracortical myelin trajectory over the lifetime

ICM in humans develops through a long process that extends into middle age and occurs in a regional and depth-dependent manner. Specifically, intracortical myelination occurs over the lifetime in a reproducible inverted "U"-shaped trajectory (Grydeland et al., 2013; Rowley et al., 2017). The amount of myelination in the cortex increases rapidly throughout adolescence and early adulthood, reaching its peak around the fourth decade. During middle life, this trajectory reaches a plateau wherein the amount of myelin in the cortex is relatively constant. Finally, in the sixth decade, the amount of myelination in the cortex experiences a rapid decline (Grydeland et al., 2013).

Although the rate of myelination is consistent across cortical depths, the time at which myelination begins and peaks differs across cortical regions. For example, the visual and cingulate association areas are the last to begin myelination but reach their peak amount of myelin earliest among cortical regions. The frontal and temporal lobes begin heavy myelination later in development and reach their peak after the cingulate cortices (Bartzokis et al., 2001). This is in contrast to motor regions, which begin heavy myelination first in the cortex but reach peak myelination last (Rowley et al., 2017; Westlye et al., 2010). This age trajectory has been assessed across all cortical depths, and the pattern remains consistent (Rowley et al., 2017).

1.2.4 Impacts of psychiatric illness on intracortical myelin

Cortical thickness and the density of neurons and glial cells within have long been neurobiological markers of interest for psychiatric illness. Extensive research has shown that cortical thinning occurs in individuals suffering from various psychiatric disorders, including bipolar disorder and schizophrenia (Hanford et al., 2016; Kuperberg et al., 2003). Previously, cortical thinning was believed to be a direct reflection of neuronal density but is now known also to reflect the density of oligodendrocytes and, thus, myelin in the cortex (Zatorre et al., 2012). Post-mortem studies assessing the density of cells in the cortex have identified that individuals with mood disorders have a lower ratio of oligodendrocytes and neurons than is observed in psychologically healthy individuals (Öngür et al., 1998). Studies assessing ICM *in vivo* have confirmed these oligodendrocyte deficits and show that myelin is disrupted in individuals with various psychiatric disorders (Bartzokis et al., 2009; Jørgensen et al., 2016). Together, these findings indicate that ICM deficits are a reproducible marker of psychiatric illness. Worsened clinical outcomes of psychiatric disorders are also predicted to be risk factors for ICM deficits. Recent studies have found that the duration of illness, age of onset, and certain medication usage are associated with bipolar disorder (Sehmbi et al., 2019). However, more research is needed in this area to confirm the direction of these relationships.

ICM deficits have been primarily shown in bipolar disorder and schizophrenia, with recent studies suggesting that these deficits extend to other disorders, including major depressive disorder (MDD) (Sacchet & Gotlib, 2017) and alcohol use disorder (Morris et al., 2022). However, the findings with respect to these disorders are limited. In schizophrenia, post-mortem histological studies assessing cortical myelination have found that the density of oligodendrocytes is decreased compared to healthy individuals, with one study estimating 22% reductions in the frontal lobe (Hof et al., 2002). These findings have been confirmed through *in vivo* imaging studies, which show that the amount of myelination, approximated based on the signal of cholesterol of myelin in the cortex, is decreased in schizophrenia (Tishler et al., 2018; Wei et al., 2020). Similar ICM deficits are observed in bipolar disorder, with post-mortem histology studies finding reductions in oligodendrocyte density in individuals with the disorder (Lake et al., 2017) and *in vivo* imaging studies finding region and depth-specific reductions in ICM related to bipolar disorder (Jørgensen et al., 2016; Rowley et al., 2015). ICM deficits in bipolar disorder are associated with psychosocial functioning (Sehmbi et al., 2022) and deficits in various domains of cognitive functioning (Sehmbi et al., 2018).

Additionally, the inverted U-shaped trajectory of the T_1-weighted (T_1w) signal is blunted in individuals with bipolar disorder (Sehmbi et al., 2019). These individuals reach their peak amount of myelination earlier than psychologically healthy individuals. In addition, the amount of myelin in the cortex at the peak is less than in individuals without psychiatric illness. This blunting of the myelin trajectory throughout the lifetime has also been observed in individuals with schizophrenia (Bartzokis et al., 2009, 2012). In these individuals, the peak amount of myelin in specific cortical regions is reached earlier than in healthy controls, with a similar blunted effect to those with bipolar disorder.

Past research has shown that brain structural deficits are widespread and found to differ across the left and right hemispheres. The lateralization of deficits in bipolar disorder is an area that has been widely debated. The literature tends to indicate that the right hemisphere is impacted more heavily by bipolar disorder. For example, one study assessing white matter abnormalities in psychiatric illness found more abnormalities in the right hemisphere of individuals with bipolar disorder (Ho et al., 2017). However, other studies oppose the propensity towards right hemisphere abnormalities by showing that individuals with bipolar disorder have increased activation in the left hemisphere in the prefrontal cortex (Altshuler et al., 2008) and cingulate cortex (Blumberg et al., 2000). These conflicting results emphasize the importance of assessing brain regions bilaterally.

1.2.5 *Ex-vivo* methods of estimating intracortical myelin

Studies assessing the myeloarchitecture of the human cerebral cortex have relied heavily on the use of post-mortem tissue. Through these studies, staining oligodendrocytes has allowed for estimations of the amount of ICM in the cortex (Carriel et al., 2017). This myelin staining has contributed to the fundamental understanding of the age trajectory of myelin that was later fortified via imaging methods (Kemper, 1994). Post-mortem cytology data shows that the rate of intracortical oligodendrocyte development increases in healthy individuals into adulthood, but in schizophrenia, this number is decreased, reaching its peak in earlier adulthood than in psychologically healthy individuals (Vostrikov et al., 2007).

These *ex-vivo* assessments have also allowed for the association between myelin amounts in the cortex and gene expression to identify markers of myelin deficits. Cortical thickness has been shown to be under extensive genetic influence, with estimates of up to 50% of individual differences in cortical thickness resulting from genetic factors (Schmitt et al., 2020). Expression of myelin-related genes is downregulated in the prefrontal cortex of individuals with bipolar disorder and schizophrenia (Tkachev et al., 2003). Also, mutations in myelin signalling genes have been found to alter the expression and functioning of proteins that produce myelin in the cortex, possibly contributing to observed deficits (Shine et al., 1992).

Post-mortem histology staining of cortical myelin has since been compared with *in vivo* imaging to confirm that observed decreases in the number of oligodendrocytes are also reflected in the tissue properties of current imaging techniques (Bock et al., 2009).

1.2.6 *In vivo* imaging to estimate intracortical myelin

Initial *in vivo* imaging of cortical myelin was done using inversion recovery (IR) and proton density (PD) MRI images to find the boundary between white matter and grey matter in the cortex (Bartzokis et al., 2009). These IR images are sensitive to the contrast created by cholesterol and take advantage of the fact that myelin contains the greatest cholesterol concentration compared to other tissue types in the cortex. IR images were used as a proxy measure of white matter within the cerebral cortex, now known to reflect myelin (Bartzokis et al., 1993). The addition of PD images was done to identify the grey matter boundary of the cortex. These image contrasts were used to identify the boundary between white and grey matter and are a proxy measure of ICM (Bartzokis et al., 2009).

Newer methods developed to map ICM include a quantitative MRI sequence that measures a parameter sensitive to myelin, including T_1 (Marques & Gruetter, 2013; Sereno et al., 2013). One such method was developed by Glasser and Van Essen, which involves creating a ratio image of T_1-weighted and T_2-weighted MRI images (T_1w/T_2w) (Glasser & Van Essen, 2011). This method of dividing one image by the other allows for correcting MRI-related image intensity bias fields and increasing the contrast-to-noise ratio of myelin. However, T_1w/T_2w is a relative measure of approximating myelin content and transmit field biases cannot be fully eliminated from the ratio image. This method also depends on the exact sequence setting used during imaging, leading to variability between studies (Nerland et al., 2021).

A more direct measure of approximating myelin is longitudinal relaxation rate (R_1), the inverse of T_1 signal intensity. Variation in R_1 has been shown to reflect water content within myelin, and comparisons between *ex-vivo* and *in vivo* studies confirm the accuracy of R_1 as a measure of myelin content (Schmierer et al., 2004). R_1 surface maps can be formed using T_1 images conducted with a qualitative sequence optimized to maximize intracortical contrast (Bock et al., 2013). These images can be reconstructed into surface maps that approximate the amount of myelin in the whole brain.

Studies comparing methods of *in vivo* myelin imaging have shown that while T_1w/T_2w and R_1 both measure myelin, the two methods are sensitive to different myelin properties. One study concludes that T_1w/T_2w signal contrast properties are preferable for cortical-based segmentation, while R_1 mapping is preferred for cohort-based studies when assessing varying cortical properties (Shams et al., 2019). For this reason, the current study utilizes R_1 surface maps with contrast optimized for myelin imaging.

1.3 Neuregulin-1

1.3.1 Neuregulin-1 and nervous system development

Neuregulins are a family of epidermal growth factor (EGF)-like membrane glycoproteins. These proteins are divided into six groups (NRG 1-6), encoded by different genes. The largest of these genes, and one of the longest in the human genome, is *NRG1* (Falls, 2003). This gene spans 2.6 million base pairs and is located on the eighth chromosome (Chou & Ozaki, 2010). The neuregulin-1 (Nrg-1) proteins encoded by this gene are involved in various functions related to the development and proper functioning of the nervous system. These proteins are involved in the proliferation of various cell types for the formation of organ tissues, including the development of neurons and glial cells in the CNS and the formation of synapses (Harrison & Law, 2006). In the CNS, Nrg-1 is involved in the proliferation and differentiation of oligodendrocytes, which form myelin sheaths. After the initial formation of the nervous systems during development, these proteins have widespread roles in cell-cell signalling and synaptic plasticity (Kataria et al., 2019). *NRG1* is expressed consistently across cortical regions and depths, but particularly, mRNA expression is increased in the prefrontal cortex (Law et al., 2004). *NRG1* transcripts are expressed in the cytoplasm of cells in the CNS where they are transcribed to express Nrg-1 proteins which are then able to impact neuronal functioning (Shamir & Buonanno, 2010).

The presence of regulatory elements in the 5' promoter region of *NRG1* allows for alternative splicing of the coding DNA, which leads to the formation of over 30 different isoforms in the human genome, categorized into six groups (type I-VI) (Kataria et al., 2019; Tan et al., 2007). Each type of Nrg-1 protein differs in its structure and function and is expressed in a tissue-specific manner (Liu et al., 2011). Although the types of Nrg-1 differ in structure and function, they all share a common EGF-like domain that allows them to bind to tyrosine kinase receptors (Falls, 2003). One class of receptors that bind to Nrg-1 is the ErbB class of tyrosine kinase receptors, particularly ErbB4, through which they regulate downstream signalling cascades and, through this, modulate synaptic transmission (Ledonne & Mercuri, 2020). This allows Nrg-1 to play a role in signalling pathways, including glutamate (Ozaki et al., 1997), GABA (Rieff et al., 1999), and acetylcholine (Liu et al., 2001). With regards to glutamate, binding of Nrg-1 to ErbB4 allows for the expression of the NR2C subunit of N-methyl-D-aspartic acid (NMDA) receptors, which is necessary for the neurotransmission of glutamate in the CNS (Ozaki et al., 1997). The *NRG1/ERBB* pathway has also been implicated in dopamine signalling, which is altered upon the knockout of the *ERBB4* gene. One study assessing transgenic mice proposes that *NRG1* gene variants that increase protein expression may contribute to white matter deficits observed in psychiatric illness. Increased excitation caused by upregulated Nrg-1 expression can cause dopamine receptors and transporters to upregulate production to produce a compensatory response that may contribute to white matter abnormalities (Roy et al., 2007). Variants of Nrg-1, through alterations in synaptic transmission, have also been shown to impact cognitive functioning in individuals suffering from psychiatric disorders (Rolstad et al., 2015; Stefanis et al., 2007).

1.3.2 Neuregulin-1 and psychiatric illness

NRG1 has been identified as a risk gene for the development of various adverse outcomes, including psychiatric illness. This relationship was first identified in individuals with schizophrenia, and since then, candidate-gene studies have replicated findings that *NRG1* variants confer risk for the disorder (Li et al., 2006). Family studies conducted on individuals with schizophrenia and their unaffected relatives have found a shared genetic variation in the *NRG1* gene that contributes to the heritability of the disorder (Mostaid et al., 2016). The genetic variants associated with schizophrenia are most often found in the *NRG1* type II and IV isoforms and often in the upstream regulatory region of the gene, leading to altered expression levels (Harrison & Law, 2006). *NRG1* was first identified as a risk gene for schizophrenia in a study that assessed the impact of one haplotype on schizophrenia risk in an Icelandic population (Stefansson et al., 2002). This haplotype, named HAP_{ICE}, includes 12 SNPs and four microsatellite markers that were found to increase susceptibility to schizophrenia. This haplotype has since been confirmed in various populations, including Scottish (Stefansson et al., 2003), Dutch (Bakker et al., 2004), Japanese (Fukui et al., 2006), and Indian (Kukshal et al., 2013).

Research on the risk of *NRG1* genetic variation for developing psychiatric disorders has extended beyond schizophrenia. *NRG1* has also been found to contribute to the risk of developing bipolar disorder (Cao et al., 2014) and MDD (Wen et al., 2016). In addition to mood disorders, recent research has indicated a potential role of *NRG1* variants in the risk of anxiety disorders, including post-traumatic stress disorder (PTSD) (Luo et al., 2020). *NRG1* has also been associated with psychiatric symptoms, particularly symptoms of psychosis, in individuals with schizophrenia and bipolar disorder (Goes et al., 2009; Hall et al., 2006).

1.3.3 Neuregulin-1-associated structural and functional brain changes

Variation in the *NRG1* gene is associated with alterations in the structure and functional connectivity of the brain. Structurally, polymorphisms in *NRG1* have been shown to decrease white matter integrity and density both in individuals with and without a history of psychiatric illness (Duan et al., 2021; McIntosh et al., 2008; Winterer et al., 2008). In schizophrenia, the HAP_{ICE} haplotype has been associated with decreased white matter volume in regions of the cortex, brainstem and cerebellum (Cannon et al., 2012). SNPs located in the gene have been associated with decreased white matter integrity and density in individuals with schizophrenia, bipolar disorder and MDD compared to psychologically healthy individuals (Duan et al., 2021). *NRG1* variants are also associated with decreased grey matter volume in healthy individuals (Barnes et al., 2012).

Alterations in functional connectivity have also been associated with *NRG1* variants in bipolar disorder and schizophrenia. Specifically, individuals carrying *NRG1* variants show increased activation in cortical regions associated with bipolar disorder and schizophrenia, which is only observed in individuals with these diagnoses (Mechelli et al., 2008). Other studies have found that *NRG1* variants show decreased functional connectivity in the prefrontal cortex and limbic system (Marlinge et al., 2014).

1.3.4 Neuregulin-1 rs6994992 polymorphism

One marker from the HAP_{ICE} haplotype that has received particular attention with respect to psychiatric disorders is the single nucleotide polymorphism rs6994992, also known as SNP8NRG243177. Since the discovery of the haplotype, the relationship between rs6994992 and schizophrenia has been replicated in multiple studies, showing the consistency of the relationship (Li et al., 2006). This marker has been isolated as a major susceptibility factor for adverse outcomes of psychiatric illness, including the presence of structural and functional abnormalities in the cerebral cortex (Barnes et al., 2012; Zhang et al., 2019) and deficits in cognitive functioning (Stefanis et al., 2007).

Rs6994992 is a single nucleotide substitution polymorphism in the promoter region of type IV *NRG1* located 1.2 kb upstream of the transcriptional start site (Law et al., 2006). In individuals with this polymorphism, a cytosine (C) nucleotide is substituted by a thymine (T) nucleotide. Substitution of the T allele in the promoter region increases the expression of type IV Nrg-1 mRNA (Moon et al., 2011). Studies performed on post-mortem human brain tissue have found that heterozygous individuals (genotype C/T) exhibit 21% more Nrg-1 mRNA than individuals homozygous for the common allele (genotype C/C). Individuals who are homozygous for the minor allele (genotype T/T) exhibit the greatest expression of Nrg-1 mRNA, with 49% more than those that are homozygous for the common allele (Law et al., 2006). This indicates that the rs6994992 polymorphism exhibits an allele dose-dependent effect, where with a greater number of risk alleles present, the expression increases. These allele dosage effects have also been found for adverse outcomes of rs6994992. Specifically, one study assessing functional connectivity in individuals with the rs6994992 genotype found that connectivity was disrupted in individuals with one copy of the risk allele (C/T) and increasingly disrupted in those with two copies (T/T) (Zhang et al., 2019).

1.3.5 Risk outcomes of rs6994992

Research has shown that individuals carrying a T allele at the rs6994992 locus are more susceptible to developing psychiatric disorders, including schizophrenia (Li et al., 2006), bipolar disorder (Green et al., 2005), MDD (Moon et al., 2011), and psychotic symptoms (Bousman et al., 2014; Hall et al., 2006). The risk allele is associated with worse functional and neurobiological outcomes for individuals with these disorders than individuals without psychiatric diagnoses (Stefanis et al., 2007; Zhang et al., 2019).

The risk genotype of rs6994992 has been associated consistently with structural and functional brain changes. In individuals with schizophrenia, the T/T genotype has been associated with decreased prefrontal activation (Hall et al., 2006). This risk for adverse outcomes extends to unaffected family members of individuals with schizophrenia, indicating that these adverse outcomes have a genetic basis. In these family members, the rs6994992 risk allele has been significantly associated with increased psychosocial stress, among other outcomes (Kéri et al., 2009). For psychologically healthy individuals, the presence of the risk allele is also associated with abnormalities in the structure and function of the brain. Previous studies have found decreases in white matter integrity in thalamic radiation (Sprooten et al., 2009) and medial frontal white matter (Winterer et al., 2008). Research assessing structural changes in healthy individuals shows decreased white and grey matter volumes in various regions of the cerebral cortex (Barnes et al., 2012) and reduced white matter density in the internal capsule (McIntosh et al., 2008). Functional studies have also found that the T allele is associated with disruption of network connectivity modulation (Lubeiro et al., 2017) and disruption of whole-brain functional connectivity (Zhang et al., 2019).

Although the findings assessing the impact of rs6994992 in schizophrenia have been consistently replicated, the findings concerning bipolar disorder and other mood disorders are conflicting (Li et al., 2006). Some studies failed to find a significant association between the risk allele and bipolar disorder (Díez et al., 2014; Georgieva et al., 2008). In contrast, others found that the rs6994992 risk genotype is significantly associated with bipolar disorder (Green et al., 2005; Gutiérrez-Fernández et al., 2014). As for research regarding structural and functional changes related to the rs6994992 genotype, some studies have found no significant associations between the risk genotype and various structural brain changes (Suarez-Pinilla et al., 2015) despite others finding that the T allele significantly alters the structure and functional connectivity of the cortex (McIntosh et al., 2008; Zhang et al., 2019). This heterogeneity of results emphasizes the need for further study to elucidate the role that neuregulin-1 plays in the structural development of the cerebral cortex.

1.4 Salience Network

As mentioned previously, individuals with bipolar disorder display functional connectivity abnormalities in specific brain areas that contribute to deficits in functioning, including cognition. Three primary networks are involved in neurocognitive processing: the default mode network, the central executive network, and the salience network. One theory of neurocognitive dysfunction, known as the triple network model, predicts that abnormalities in one of these networks lead to dysregulation of all three networks and overall deficits in cognitive functioning (Menon, 2011). Dysfunction in these three networks has been associated with neuropsychiatric disorders, possibly contributing to deficits in neurocognition that are commonly observed in these disorders. In one of these networks, the salience network, deficits in various regions have been associated with bipolar disorder (Vargas et al., 2013; Wessa et al., 2007) and schizophrenia (Chen et al., 2016; White et al., 2013). The salience network serves as a mediator between the default mode network and the central executive network, controlling the activation of each network by assessing the level of subjective salience of a stimulus and dictating the level of attention necessary (Goulden et al., 2014; Sridharan et al., 2008).

The salience network is anchored in the dorsal anterior cingulate cortex (dACC) and the anterior insular cortex (AIC), also known as the fronto-insular cortex (FIC), with nodes that extend into subcortical regions of the brain, including the thalamus, hippocampus, periaqueductal gray and amygdala (Seeley et al., 2007). Through activating these regions, the salience network can access working memory to determine where to supply attentional resources (Luo et al., 2014). The regions of the salience network thus contribute to emotion processing and regulation of autonomic functions by integrating sensory information with internal bodily state signals (Seeley et al., 2007). The regions of the salience network, particularly the dACC and AIC, are functionally connected with each other more than any other brain regions. This coordination between salience network regions allows information to be communicated to surrounding brain areas. The dACC and AIC are functionally connected to brain regions involved in cognition and other higher-order processes but show negative functional connectivity with regions involved in primary motor control (Cauda et al., 2011; Margulies et al., 2007). This disconnect in function is reflected by a difference in structure wherein the ACC and AIC are two of the most lightly myelinated regions of the cerebral cortex in contrast to the primary motor cortex, which is one of the most heavily myelinated (Glasser & Van Essen, 2011).

The salience network has been implicated as a potentially interesting network of brain regions implicated in psychiatric illnesses, including bipolar disorder. Past research has found that connectivity between the default mode network and the salience network is disrupted in individuals with bipolar disorder (Gong et al., 2019; Lopez-Larson et al., 2017). Assessments of cortical structure have found that cortical regions of the salience network, including the ACC and AIC, show grey matter deficits in individuals with schizophrenia (Bennett, 2011) and healthy individuals (Barnes et al., 2012). Decreased white matter integrity has also been found in the ACC in individuals with schizophrenia (Wang et al., 2009) and white matter volume in healthy individuals (Barnes et al., 2012).

Similar to how cortical thickness is under genetic influence, these observed deficits in white and grey matter are altered by genetic variation. *NRG1* is one gene contributing to structural abnormalities observed in individuals with and without psychiatric illness. Notably, the rs6994992 risk allele has been associated with decreased white and grey matter volumes in the ACC (Barnes et al., 2012), and a different risk SNP of *NRG1*, rs35753505, has shown abnormal white matter integrity in the ACC (Wang et al., 2009).

Due to their role in psychiatric illness and relationship to *NRG1* gene variants, the cortical regions of the salience network are potentially interesting to consider as regions of interest for assessing the genetic impacts of bipolar disorder on changes in ICM.

1.5 Aims and Hypotheses

The current study attempts to connect past research done on the role of bipolar disorder in intracortical myelination to recent findings on the detriment of neuregulin genetic variation toward cortical development. This study seeks to determine the role of age, bipolar disorder diagnosis and NRG1 rs6994992 genotype on intracortical myelin in the cortical regions of the salience network, the dACC and AIC. In particular, this study identifies the role of the rs6994992 genotype in the relationship between bipolar disorder and intracortical myelination. Additionally, we intend to explore whether the *NRG1* rs6994992 genotype impacts regions outside of this network.

This study seeks to answer two questions:

1) Is intracortical myelination in the cortical regions of the salience network (dACC and AIC) predicted by age, bipolar disorder diagnosis, and rs6994992 genotype as a moderating variable?
2) Are there additional cortical regions where ICM is predicted by age, diagnosis and rs6994992 genotype?

For the first research question, it is hypothesized that age, diagnosis and genotype will significantly predict variation in ICM and that the rs6994992 genotype will moderate the relationship between bipolar disorder and intracortical myelination in the regions of the salience network. Specifically, it is predicted that individuals carrying the T-risk allele of rs6994992 will show greater ICM deficits in the cortical regions of the salience network and that the relationship between bipolar disorder and ICM will be better explained by the consideration of the rs6994992 genotype as a moderating factor. The second research question will be a whole-brain exploratory analysis to identify additional cortical regions outside the salience network that our predictive factors of interest may impact.

The intention in assessing the moderating risk of genotype is based on findings from previous studies that assessed the impact of polymorphism genotype on an outcome measure in psychiatric illness. In the current study, rs6994992 genotype is predicted to contribute to deficits in intracortical myelination through the previously established impact of bipolar disorder. It is believed that risk polymorphisms of neuregulin in individuals with bipolar disorder, and through this, an increased expression of *NRG1,* may account for a small portion of the variation in the relationship between bipolar disorder and ICM, contributing to the observed deficits in ICM. When acting through its contributions to bipolar disorder, the rs6994992 T allele is predicted to significantly impact ICM deficits, specifically in lightly myelinated cortical regions of the salience network. By addressing these research questions, the hope is to begin elucidating the impact that neuregulin-1 genetic variation may have on intracortical myelin in bipolar disorder.

CHAPTER 2 - METHODS

2.1 Participants

77 participants with BD type I and 76 healthy controls aged 16-45 were recruited from five research sites across Canada (McMaster University, Queens University, University Health Network, Dalhousie University, and University of Calgary). Participants gave written informed consent to take part in the study. The study was approved by the ethics committees of St. Joseph's Healthcare Hamilton and Hamilton Health Sciences (Project # 20004997).

Participants were included in the study if they were i) between the ages of 16-45 and ii) female participants were premenopausal. Participants were excluded if they: i) had an unstable general medical condition, ii) had any contra-indications for MRI, iii) were pregnant or intended to become pregnant during study participation, or iv) had a history of neurological disorders, including head trauma resulting in loss of consciousness and severe migraines. Participants were included in the control group if they had no current or lifetime psychiatric conditions. Participants were included in the bipolar disorder group if: i) they had a diagnosis of BD type-1 and ii) at the time of assessment, were in a euthymic state with no changes in medications for at least two months. Participants were excluded from the bipolar disorder group if they had i) a current manic/hypomanic episode or a current major depressive episode or ii) a current comorbid psychiatric disorder except for anxiety disorders.

2.2 Study Design

Participants were invited to participate in a longitudinal study assessing various outcomes of bipolar disorder at three time points: baseline, one-year and two-year follow-ups. The current analysis focuses on information collected at the baseline visit. During the initial visit, participants were first assessed for psychiatric diagnoses and demographic information through a structured questionnaire administered by a trained research assistant. Following clinical data collection, participants completed a comprehensive neuropsychological battery to assess various domains of cognitive functioning. Afterward, T_1-weighted MRI images and peripheral blood samples were collected. If, for various reasons, a participant could only complete a portion of the study during their visit, the remaining sections were rescheduled if possible.

2.3 Clinical Assessments

The Structured Clinical Interview for the DSM-V (SCID-5) was used to determine psychiatric diagnoses (First, 2002). For participants in the bipolar disorder group, information was collected regarding the age of illness onset and the number of episodes. The duration of illness was then calculated by subtracting the age of onset from the participant's age at the study visit. The Montgomery-Åsberg Depression Rating Scale (MADRS) was administered to assess the severity of depressive symptoms (Montgomery & Åsberg, 1979). The Young Mania Rating Scale (YMRS) was administered to assess the presence and severity of mania and associated symptoms (Young et al., 1978). The

Functioning Assessment Short Test (FAST) was administered to assess functional impairment in participants with bipolar disorder (Rosa et al., 2007).

2.4 NRG1 Genotyping

2.4.1 Blood Collection

Peripheral blood was collected from participants following the MRI scan. Blood for DNA extraction was collected in tubes containing an anticoagulant agent - K2 EDTA. Blood samples were collected and processed by a trained phlebotomist. Blood collected for DNA extraction was stored at -80ºC until extraction could take place.

2.4.2 DNA Extraction

DNA was extracted from peripheral whole blood using Qiagen's QIAamp DNA Midi Kit (cat. no. 51194). 1000µL BRAND micropipettes and 1000µL pipette tips from Thermo Fisher and Axygen brands were used throughout DNA extraction. Before beginning the experiment, all buffers and reagents were prepared according to package instructions using distilled water for protease and 100% ethanol for buffers. The 2mL protocol was followed, extracting two vials of DNA for each participant, according to manufacturer instructions. Briefly, a protease enzyme was pipetted into two test tubes for cell lysis, followed by 2 mL of whole blood. For tubes that contained less than 2mL of blood, phosphate-buffered saline was added to the sample to bring the volume to 2mL. The lysing process continued by heating samples at 70ºC for 10 minutes. Following incubation, ethanol was added to the samples to aid the DNA in column binding. The samples were run through a column once in a brief centrifugation step to bind the DNA to the column filter and remove excess RNA and proteins. Two additional centrifugation steps removed residual contaminants from the column by adding two wash buffers. Finally, an elution buffer was used to remove the purified DNA from the column filter through centrifugation. DNA was re-eluted through the column to obtain the maximum concentration in a final centrifugation step. DNA was extracted from test tubes and placed into microcentrifuge tubes for long-term storage at -80ºC.

2.4.3 DNA Quantification

Following the extraction procedure and before storage, DNA was quantified using the Agilent BioTek Epoch 2 Microplate Spectrophotometer with the Take3 Multi-Volume Plate. The instrument calculated the concentration of DNA from 260 nm absorbance according to the Beer-Lambert Law (Swinehart, 1962). The 260/280 ratio was used to evaluate DNA purity, and an optical density ratio of 1.8-2.0 was used as a cut-off. Typically, ratio values lower than 1.7 indicate the presence of contaminants such as proteins. Thus, a ratio of 1.8 was considered ideal for DNA extraction, and a ratio up to 2.0 was considered sufficiently pure (Khare et al., 2014). All samples were within this purity range; thus, no samples were excluded from the final analysis due to impurity.

2.4.4 Genotyping of rs6994992

Genotyping of the *NRG1* polymorphism rs6994992 was completed using real-time polymerase chain reaction (RT-PCR). The TaqMan Predesigned SNP Genotyping Assay was used to assess allele genotype (Assay ID: C____22019_10). The primer context sequence was [**VIC/FAM**] AAGCACCATGCAGGGTTCAAGTGAA[**C/T**]GTATACTGGAGGCCAGACCTGCCCA. The assay made use of Taq polymerase for primer extension. A total reaction volume of 25μL was used containing 8ng of genomic DNA, 1.25μL of 20X assay, and 12.5μL of ThermoFisher Genotyping Master Mix (2X concentration). The cycling conditions were as follows: 10 minutes at 95ºC for enzyme activation, then 40 cycles at 95ºC for 15 seconds (denaturation) and 60ºC for one minute (annealing/extension). The RT-PCR system used in this experiment was the QuantStudio 7 Flex Real-Time PCR System, with samples loaded into a 96-well plate in triplicate.

2.4.5 PCR Procedure

Prior to the experiment, the lab bench and all equipment were cleaned using DNA*Zap* solution to eliminate potential contaminating DNA from surfaces (Applied BioSciences). DNA samples were thawed, vortexed and centrifuged at 800xg for one minute before dilution. Serial dilutions were performed on DNA samples with a starting volume of 10μL taken from each DNA sample. Two sets of dilutions were completed to achieve a final amount of 8ng of DNA in a volume of 1.25 μL and a final concentration of 0.2 ng/μL of DNA in the reaction volume of 25μL, as recommended by the TaqMan SNP Assay Procedure. Nuclease-free water was used for all dilutions of DNA and assays. Samples were loaded onto a 96-well plate in triplicates. Each plate included a negative no-template control to allow for comparison of fluorescence from wells containing template DNA. Gilson brand micropipettes of various volumes and corresponding Gilson pipette tips were used throughout the PCR procedure.

2.5 Magnetic Resonance Imaging (MRI)

Whole-brain, 3D magnetic resonance images (MRIs) were collected to produce longitudinal relaxation rate (R_1) maps of each subject's brain. These R_1 maps were then used to reconstruct cortical surfaces for all ICM analyses. Images were collected on 3 Tesla MRI systems at each of the sites which are described in Table 1.

Table 1. MRI scanner specifications for each research site included in the analysis

This table outlines the MRI scanners used at each site in this study, the software used on each scanner, and the details of the radiofrequency coil.

Site	Vendor	Scanner/ Software Version	Transmit Radiofrequency Coil	Receive Radiofrequency Coil
McMaster	General Electric (GE)	Discovery 750 version 25.0	Body Coil (GE)	32-channel phased-array head coil (MR Instruments)
Dalhousie	General Electric	Discovery 750 version 25.0 R02	Body Coil (GE)	32-channel phased-array head coil (MR Instruments)
Queens	Siemens	Tim Trio version VB19A	Body Coil (Siemens)	32-channel phased-array head coil (?)
Calgary	General Electric	Discovery 750 version 25 R02	Body Coil (GE)	12-channel phased-array neurovascular coil (GE)
University Health Network	Siemens	Prisma version syngo MR E11	Body Coil (?)	32 channel phased-array head coil (?)

2.5.1 Anatomical Reference Imaging

A 3D inversion-recovery gradient-echo T_1-weighted anatomical image (*Anatomical*) with 1 mm isotropic resolution was collected at each site to be used for registering and segmenting images.

For GE sites, the following sequence was conducted: (3D BRAVO sequence) [Inversion time = 450 ms, TE = 3.1 ms, TR in acquisition block = 7.9 ms, flip angle in acquisition block = 12º, field of view (FOV) = 24.0 x 24.0 x 18.0 cm, matrix = 240 (readout) x 240 (first phase encode) x 180 (second phase encode), centric phase encoding, Autocalibrating Reconstruction for Cartesian imaging (ARC) parallel imaging factor of 2 in the second phase encode direction, Number of averages = 1, time = 5 min 32 s].

For Siemens sites, the following sequence was conducted: (tfl sequence) [Inversion time = 900 ms, TE = 3.0 ms, TR in acquisition block = 7.1 ms, flip angle in acquisition block = 9º, field of view FOV = 25.6 x 25.6 x 17.6 cm, matrix = 256 (readout) x 256 (first phase encode) x 176 (second phase encode), linear phase encoding, GRAPPA parallel imaging factor of 2 in the second phase encode direction, Reference lines = 32, Number of averages = 1, time = 5 min 30s].

2.5.2 Images for R_1 Maps

Two images were collected to calculate R_1 maps. The first was a 3D inversion-recovery gradient echo image (*Inversion*) with 1 mm isotropic resolution optimized to maximize intracortical contrast and the second was a 3D gradient echo image with 1mm isotropic resolution with no inversion pulse optimized to minimize intracortical contrast (*No_Inversion*).

The *Inversion* images at GE sites were conducted as follows: (3D BRAVO) [Inversion time = 1100 ms, time between end of acquisition block and next 180º pulse = 1000 ms, TE = 3.1 ms, TR in acquisition block = 7.6 ms, flip angle in acquisition block = 12º, FOV = 24.0 x 18.0 x 24.0 cm, matrix = 240 (readout) x 180 (first phase encode) x 240 (second phase encode), centric phase encoding, ARC factor 2 in second phase-encoding direction, Number of averages = 1, time = 5 min 53 s]. Each hemisphere was imaged separately to increase intracortical contrast as this reduced the matrix dimension in the first phase-encoding direction in the sequence allowing for a shortened acquisition block following the inversion pulse. This is analogous to using multiple segments in a magnetization-prepared rapidly acquired gradient echo sequence (MP-RAGE) (Deichmann et al., 2000), where the shorter acquisition block improves contrast. The reduced FOV was applied in this study as a true MPRAGE sequence was not available on our scanner. The long TD in the sequence provided increased intracortical contrast (Bock et al., 2013). Each hemisphere was imaged twice to increase the contrast-to-noise ratio. The four images took 24 minutes in total to acquire. Each of the four separate images was registered to the *Anatomical* reference image via a 6-parameter rigid transformation with sinc resampling using the FLIRT tool in FSL (Jenkinson et al., 2012) Version 5.0

(fsl.fmrib.ox.ac.uk/fsl/). The magnitude images were then summed to create the final image of the whole head.

At Siemens sites the *Inversion* images were conducted as: (tfl sequence) [Inversion time = 1100 ms, time between end of acquisition block and next 180º pulse = 988 ms, TE = 2.0 ms, TR in acquisition block = 6.1 ms, flip angle in acquisition block = 12º, FOV = 25.6 x 25.6 x 17.6 cm, matrix = 256 (readout) x 256 (first phase encode) x 176 (second phase encode), linear phase encoding, GRAPPA parallel imaging factor of 2 in the second phase encode direction, Reference lines = 32, Number of averages = 1, time = 8 min 14 s]. Two brain images were collected for a total imaging time of approximately 16 minutes and registered to the *Anatomical* reference image via a 6-parameter rigid transformation with sinc resampling using the FLIRT tool in FSL. The magnitude images were then summed to create the final image of the whole head.

The *No_Inversion* images at GE sites were conducted as: (SPGR sequence) [TE = 3.1 ms, TR = 7.9 ms, flip angle = 4º, field of view (FOV) = 24.0 x 24.0 x 18.0 cm, matrix = 240 (readout) x 240 (first phase encode) x 180 (second phase encode), linear phase encoding, ARC parallel imaging factor of 2 in the second phase encode direction, Number of averages=1, time = 5 min 32 s].

At Siemens sites, these *No_Inversion* images were conducted as (SPGR sequence) [TE = 3.1 ms, TR = 6.1 ms, flip angle = 4º, field of view FOV = 25.6 x 25.6 x 17.6 cm, matrix = 256 (readout) x 256 (first phase encode) x 176 (second phase encode), linear phase encoding, GRAPPA parallel imaging factor of 2 in the second phase encode direction, Reference lines = 32, Number of averages = 1, time = 2 min 29 s].

2.5.3 Transmit B_1 field maps

Images were collected to create transmit B_1 field maps (B_1^+*_map*). The GE B_1^+ maps were created using the Bloch-Siegert method (Sacolick et al., 2010) and the Siemens maps were created using two 2D echo-planar images (EPI) at flip angles of 60º and 120º respectively.

At GE sites, the B_1 map sequence was: [TE = 12.3 ms, TR = 16 ms, Flip angle = 15º, FOV = 24.0 x 24.0 x 17.6 cm, matrix = 64 (readout) x 64 (first phase encode) x 36 (slices), Number of averages = 1, time = 2 min 18 s]. The B_1^+ map is calculated on the scanner and the outputs are the B_1^+ map and a magnitude image in the same space.

At Siemens sites the sequence was: (ep_seg_se) [TE = 46 ms, TR = 5000 ms, EPI factor = 9, echo spacing = 4.2 ms, Flip angle = 60º and 120º, FOV = 25.6 x 25.6. x 14.4 cm, matrix = 64 (readout) x 64 (first phase encode) x 36 (slices), number of averages = 1, time = 2 min 50 s to acquire images at both flip angles].

Both the 60º and 120º images were registered to *Anatomical* via a 6-parameter rigid transformation with sinc resampling using the FLIRT tool in FSL. The two images were used to create *B_1^+_map* using the method described in (Boudreau et al., 2017).

Following the imaging and post-processing above, *Anatomical*, *Inversion*, *No_Inversion*, and *B_1^+_map* were all in scanner space, rigidly aligned to *Anatomical*. *Anatomical* was then rigidly aligned to the MNI_152 atlas (Fonov et al., 2009) via a 6-parameter rigid transform with sinc resampling. The calculated transform was applied to *Inversion*, *No_Inversion*, and *B_1^+_map* with sinc resampling to ensure that each subject's images were in the same orientation. We will call this space *MNI_152_rigid*.

2.5.4 R_1 Map Creation

To create the R_1 maps, look up tables (LUTs) were calculated based on numerical simulations of the Bloch equations for the sequences used to create the *Inversion* and *No_inversion* images on either the GE or Siemens MRIs.

This uses a single-pool model consisting of the transverse magnetizations of the water pool (M_X^A, M_Y^A), the longitudinal magnetizations of the water pool (M_Z^A).

$$\frac{dM_X^A}{dt} = -R_{2A}M_X^A - 2\pi\Delta M_Y^A \tag{1}$$

$$\frac{dM_Y^A}{dt} = -R_{2A}M_Y^A + 2\pi\Delta M_X^A - \omega_1 M_Z^A \tag{2}$$

$$\frac{dM_Z^A}{dt} = R_{1A}(M_0^A - M_Z^A) + \omega_1 M_Y^A \tag{3}$$

The evaluation of this set of coupled equations requires the knowledge of the following variables: the equilibrium longitudinal magnetization of the free water pool (M_0^A), the longitudinal magnetization relaxation rates R_{1A} ($1/T_{1A}$), the transverse magnetization relaxation rates R_{2A}, and the intensity of the applied RF field (ω_1). This can be converted into an evolution matrix in the form:

$$E = \begin{bmatrix} -R_{2A} & -2\pi\Delta & 0 \\ 2\pi\Delta & -R_{2A} & -\omega_1 \\ 0 & \omega_1 & -R_{1A} \end{bmatrix}$$

2.5.5 RF Excitation, Readout, and Gradient Spoiling

Simulations were run over 201 isochromats, as that was previously suggested to be a sufficient number to provide stable results when tracking spoiling and spin diffusion (Yarnykh, 2010). We assume that all isochromats occupy a single voxel and lie at equally spaced points along the readout direction, each with a magnetization vector $M_t = [\, M_X^A; M_Y^A; M_Z^A]$.

RF spoiling with phase increment ϕ, and excitation by flip angle α, was calculated using a rotational matrix for the water pool:

$$R(\alpha,\phi) = \begin{bmatrix} cos(\alpha) + (1 - cos(\alpha))cos^2(\phi) & (1 - cos(\alpha)) * sin(\phi) * cos(\phi) & -sin(\alpha) * sin(\phi) \\ (1 - cos(\alpha)) * sin(\phi) * cos(\phi) & cos(\alpha) + (1 - cos(\alpha)) * sin^2(\phi) & sin(\alpha) * cos(\phi) \\ sin(\alpha) * sin(\phi) & -sin(\alpha) * cos(\phi) & cos(\alpha) \end{bmatrix}$$

The phase is incremented with each excitation pulse, using an incremental value ϕ_0, calculated as:

$$\phi_t = \phi_{t-1} + (j-1)\phi_0, j = 1, 2, 3, \ldots$$

The RF spoiling increment was set to 117 degrees for GE, and 50 degrees for Siemens. The resulting magnetization following an excitation pulse is:

$$M_t = R(\alpha, \phi) * M_{t-1}$$

Gradient spoiling and spin diffusion were calculated using the complex valued combination of M_X^A M_Y^A ($M_\perp$). Gradient spoiling resulted in an updated $M\perp$:

$$\mathrm{M}_{\perp,\mathrm{t}} = \mathrm{M}_{\perp,\mathrm{t}-1} * \exp(i\gamma G x t_G)$$

Where γ is the gyromagnetic ratio, *G* is the gradient field strength (mT/m), *x* is the distance from the reference point (where *G* = 0, varying across the isochromats), and t_G is the duration of the spoiling gradient.

Spin diffusion was calculated using the previously proposed circular convolution of isochromatic magnetization (Gudbjartsson & Patz, 1995a, 1995b). This involves convolving $M_\perp$ with a correction kernel c(*x*,*t*):

$$c(x,t) = \frac{1}{\sqrt{4\pi D t}} \exp\left(\frac{-x^2}{4Dt} - \frac{\gamma^2 G^2 t^3}{12} + \frac{i\gamma G x}{2t}\right)$$

Where *t* is the timestep that the diffusion occurs over, and *D* is the diffusion coefficient, which is a property of the tissue. The diffusion coefficient was assumed to be 1e-3 mm^2/s. Spin diffusion was modelled along the single gradient spoiling direction, if the time step was >3 ms and considered to be negligible for smaller time steps. If a gradient was applied as a portion of a longer timestep, then the gradient strength was normalized to provide the same area over the larger time step. Diffusion of M_Z^A was also employed, using the same convolution method, while setting G = 0.

After the excitation, spoiling and spin diffusion calculations, we calculate the spin evolution using the evolution matrix (E) derived from the Bloch-McConnel equations, with saturation and excitation variables set to 0. The magnetization at the next time step can be calculated as:

$$M_{t+\Delta t} = \exp(E\Delta t)\, M_t + E^{-1}(\exp(E\Delta t) - \mathrm{I}) \cdot B$$

Where E is the evolution matrix, *t* is the timestep, I is the identity matrix, and *B* = [0; 0; $R_{1A}M^A_{Z(t=0)}$; $R_{1B}M^B_{Z(t=0)}$; 0].

2.5.6 Look-up Table Generation

The above simulations were solved over a range of T_1 and B_1^+ values for the *Inversion* and *No_inversion* sequences for both scanner vendors (GE and Siemens). A gradient spoiling strength of 24 mT/m was assumed for GE, and 22 mT/m for Siemens, with an effective spoiling duration of 1.8 ms. The inversion efficiency was set to 96% for the inversion pulses. All scans were simulated for five seconds of dummy scans. As simulations of RF spoiling and gradient spoiling can provide fluctuations in values, the signal was averaged over the values extracted from the 20 subsequent simulated TRs.

The *Inversion* sequence on the GE scanner used centric encoding, with the image value taken as the first simulated excitation pulse in the readout. For the Siemens *Inversion* sequence, the signal was taken as the signal value at the midpoint of the readout (176/2). The simulated signal value was the magnitude of the XY magnetization components following the application of the excitation pulse.

One site (University Health Network) had different TE's for the *Inversion* and *No_inversion* scans. To mitigate this issue, the simulated signals were multiplied by exp(-TE / T_2*), where T_2* was assumed to be 60 ms. The TE for the *No_inversion* and the *Inversion* scans was 2.96 ms and 2.01 ms, respectively, at this site.

The LUT was built to take the ratio of the *Inversion* to *No_inversion* scans and the B_1^+*_map* as input, returning a T_1 value. The R_1 map was calculated as $1/T_1$ and was in *MNI_152_rigid* space.

2.5.7 Brain Volume Segmentation and Cortical Surface Reconstruction

Anatomical in *MNI_152_rigid* space was used as input to the Freesurfer image analysis suite, which is documented and freely available for download online (http://surfer.nmr.mgh.harvard.edu/). This segmented regional brain volumes (Fischl et al., 2002) in each subject's brain according to the aseg atlas. Region-of-interest (ROI) measurements of R_1 in the various regions identified by Freesurfer in *Anatomical* were calculated by averaging over voxels in each subject's corresponding *R_1_map* in Matlab Version 9.12.0 (https://www.mathworks.com/products/matlab.html). During the procedure, brainmask.mgz was manually inspected and edited in each subject to remove dura matter that was originally included in the mask such that the pial/CSF boundary was properly identified.

Anatomical was further used to reconstruct a middle-depth cortical surface following the methods outlined for the Human Connectome Project (Glasser et al., 2013). Briefly, the pial and white matter surfaces from Freesurfer in *MNI_152_rigid* space were used as inputs to the surface-average command in the Connectome Workbench version 1.3.2 (https://www.humanconnectome.org/software/connectome-workbench) to generate a middle-depth surface in *MNI_152_rigid* space. The R_1 values from *B_1^+_map* in *MNI_152_rigid* space were then sampled onto the middle-depth surface using the -volume-to-surface-mapping command in Connectome Workbench using the myelin-style approach with a sigma of 2.3. The values were transferred to the corresponding middle-depth surface in the standard FS_32k_LR surface space. Finally, mean ROI R_1 values for cortical regions defined from a multi-modal parcellation of the cerebral cortex (Glasser et al., 2016) were calculated for each subject using the -cifti-parcellate command in the Connectome Workbench.

2.5.8 Ratio Scaling Cortical Corrections

Two participants completed a scan at each site within two months of time, known as the travelling heads scans. Examining the travelling heads scans, R_1 values from the Siemens sites most closely resembled previous findings using 3.0T scanners (Bojorquez et al., 2017; Karakuzu et al., 2022; Marques et al., 2010; Weiskopf et al., 2013; Wright et al., 2008). Hence, harmonization techniques were employed to match the GE scanners' data to the Queens site.

For comparisons across sites, the travelling head *Anatomical* images were non-linearly registered to the MNI152 standard space and transforms were applied to all images. These images will be referred to as $MNI152_{NL}$ space. A set of R_1 maps were created by multiplying a scaling factor to the T_1wHC/T_1wHC ratio maps in both *MNI_152_NL* and *MNI_152_rigid* space. These scaling factors ranged from 0.82 to 1.10 for the McMaster site and 0.82 to 1.00 for both Dalhousie and Calgary.

For the GE sites, mean cortical surface ROI R_1s were calculated for each of the scaled R_1 maps from the travelling head scans. Histograms of 360 mean R_1s, one for each ROI, were compared. The scaling factor that led to the most overlap with the Siemens site was chosen as an optimal cortical scaling factor. Optimal scaling factors were 0.98 for McMaster and 0.90 for Dalhousie and Calgary. Mean cortical R_1s computed after scaling the T_1wHC/T_1wLC ratio maps by their site-specific scaling factors were used in cortical analyses. Ratio scaling was completed in MATLAB version 9.12.0.

2.5.9 Regions of Interest

The whole brain myelin signal was parcellated into regions of interest using the MSMAll atlas, with each hemisphere divided into 180 regions (Glasser et al., 2016). Based on past research, the dorsal anterior cingulate cortex (dACC) and the anterior insular cortex (AIC) were selected as regions of interest to focus on in this analysis. Six ROIs from the MSMAll atlas were averaged to represent the dACC: 33pr, a24pr, p32pr, d32, a32pr, p24. Four regions from the atlas were averaged to represent the AIC: MI, Pir, AVI, and AAIC. ROIs were averaged separately for the left and right hemispheres to observe lateralization effects. The primary motor cortex was selected as a negative control region to compare the results with that of the salience network regions. This region was selected due to its high amount of myelination compared to other brain regions and because it has been shown to be functionally disconnected from the regions of the salience network (Glasser & Van Essen, 2011). From the MSMAll atlas, the primary motor cortex was parcellated and represented as area 4.

2.6 Statistical Analyses

2.6.1 Missing Data

Multiple participants were excluded from the final analysis if data were missing for any of the included outcomes. Multiple whole-blood samples were missing and unable to be retrieved for DNA extraction and genotyping. For the participants with additional time points (n=21), the whole blood from a follow-up visit was used to replace missing baseline samples. This was done because DNA was assessed for *NRG1* SNP genotype, a factor that does not change with time and, thus, would be the same at each visit. Participants were excluded from the final analysis (n=4) if they were missing baseline whole blood samples and did not have a follow-up visit available with blood samples to use for the analysis. For imaging, participants were excluded if MRI images were incomplete or the quality was unusable for processing (n=2). Additionally, after data collection, multiple participants were found to have ineligible comorbidities or a primary diagnosis of bipolar disorder type II and thus were excluded (n=7). After excluding these participants, the final analyses consisted of 142 participants, 67 with diagnoses of bipolar disorder type I and 75 healthy controls.

2.6.2 Demographic and Clinical Analyses

Bipolar disorder and healthy control groups were assessed for differences in various demographic variables, including age, sex, and years of education. Comparisons were also made for clinical variables, including the severity of depressive symptoms (measured by MADRS), manic symptoms (measured by YMRS), and a measure of overall functioning (measured by FAST). For continuous variables, independent samples t-tests were conducted to determine whether variables were significantly different between the two groups. Categorical variables were assessed for differences using the Chi-square test. Significance was reported as p-values, with a threshold of $p<0.05$ indicating statistical significance.

2.6.3 Allelic Separation Analysis

PCR plates were analyzed using Applied Biosciences Design and Analysis version 2.6 (https://www.thermofisher.com/ca/en/home/technical-resources/software-downloads/quantstudio-6-7-pro-real-time-pcr-system.html) to determine participants' genotypes. All PCR data was added to the Thermo Fisher Connect Platform to compile genotype information and export the allelic discrimination plot. Once analyzed, the genotyping data was exported and assessed for significant differences using R version 4.2.3 (https://cran.rstudio.com/).

Due to a small number of participants with the T/T genotype in the bipolar disorder group (n=4), a dominance model of allelic discrimination was chosen, combining all participants carrying a T allele into one group (C/T, T/T) and comparing to individuals not carrying the T allele (C/C genotype). This method is similar to past studies assessing the impact of rs6994992 genotype on brain structural changes (Barnes et al., 2012; Wang et al., 2009). A Chi-square test was performed to assess whether the frequency of the C/C genotype and C/T, T/T genotypes significantly differed between bipolar disorder and healthy control subjects. Hardy-Weinberg equilibrium was assessed for each group separately and for the whole sample using the Chi-square test for sample sizes > 5 and Fisher's exact test for sample sizes < 5.

2.6.4 *A priori* analysis - age, bipolar disorder, and genotype as predictors of ICM

Multiple linear regressions were used to predict changes in ICM with age, diagnosis, and genotype included as predictive factors. Sex was not included as a predictive factor of ICM because past research has shown that sex does not significantly impact ICM (Rowley et al., 2017).

ICM ~ age + diagnosis + genotype

All assumptions of linear regression were evaluated before analyzing the data to ensure each assumption was met. The assumption of linearity was evaluated by examining the residuals versus predicted values. The Shapiro-Wilk test was used to assess the normality of residuals. The non-constant error variance test was used to evaluate the homoscedasticity assumption. The Durbin-Watson test was used to assess for significant autocorrelations, thus testing the independence assumption.

The regression analysis was conducted initially to predict changes in ICM in the dACC and AIC in two separate regression models, with R_1 signal intensity averaged across multiple ROIs corresponding to each region and separate models for each hemisphere. The analysis was then performed again for the primary motor cortex to use as a negative control comparison. For each of these six regression analyses, an additional model was created, which included an interaction term between diagnosis and genotype.

ICM ~ age + diagnosis + genotype + diagnosis*genotype

An analysis of variance (ANOVA) was then conducted, comparing the model with and without the inclusion of the interaction term. This was done to determine whether genotype significantly moderates the relationship between group diagnosis and ICM. All statistical analyses were performed in R version 4.2.3 (https://cran.rstudio.com/). A significance level of $p<0.05$ was required for significance in this hypothesis-driven analysis. The effect size was calculated for significant predictor variables, measured using partial eta squared (η_p^2).

2.6.5 Exploratory analysis of cortical regions associated with age, diagnosis and genotype

An exploratory analysis was performed on the remaining regions of interest to identify if ICM in any cortical regions outside the salience network was significantly predicted by age, diagnosis and genotype. The ROIs were averaged into 22 regions, bilaterally for a total of 44 regions, determined by the MSMAll atlas according to the functional connectivity of regions and structural architecture (Glasser et al., 2016). ROIs corresponding to the dACC, AIC, and primary motor cortex included in the hypothesized analyses were excluded from the sections in this exploratory analysis. A linear regression was conducted for each region with ICM as the response variable and age, diagnosis, and genotype as predictor variables. P-values were corrected for multiple comparisons. A threshold of 0.00114 ($\alpha = 0.05/44$ tests) was used to determine statistical significance. Partial eta squared (η_p^2) is reported as a measure of effect size.

2.6.6 Power Analysis

A power analysis was completed on each linear regression model for the hypothesis and exploratory analyses. This was done using the f^2 power test for linear models. Cohen's f^2 was calculated for each model's predictor terms and inputted as the measure of effect size for the power analysis. A significance level of 0.05 was used for hypothesized linear models and 0.00114 for exploratory models.

CHAPTER 3 - RESULTS

3.1 Participant Characteristics

The final analysis included 67 participants in the bipolar disorder group and 75 participants in the healthy control group. The demographic and clinical characteristics of the sample are summarized in **Table 2**. The average age for bipolar disorder participants was 32.2 years (SD = 7.6, range 19-45), and for healthy controls was 27 years (SD = 7.2, range 16-42). The bipolar disorder and control groups did not significantly differ for sex ($p = 0.926$) or years of education ($p = 0.09$). However, the bipolar disorder group had a higher average age than the control group ($p < 0.001$). Due to this difference between groups, age was included as a variable in all models assessing ICM. For clinical variables, participants in the bipolar disorder group had significantly higher scores than healthy controls for depressive symptoms (MADRS score; $p < 0.001$), manic symptoms (YMRS score; $p < 0.001$), and overall functioning (FAST score; $p < 0.001$).

Table 2. Demographic and clinical characteristics of study participants, separated by group

Summary of demographic and clinical characteristics according to group status (bipolar disorder and healthy controls). Mean ± standard deviation values are reported for continuous variables. Sex is reported as the number and percentage of female participants. Genotype is reported as a ratio of individuals with C/C genotype to those carrying a T allele (C/T, T/T). The difference between bipolar disorder and healthy controls for each characteristic are reported with test statistics (t or χ^2) and p-values. **(*)** indicates significant differences at a level of 0.05.

Characteristic	**Bipolar disorder type I**	**Healthy control**	**Test statistic**	***p* value**
N	67	75		
Age, yr	32.2 ± 7.6	27 ± 7.2	$t = 4.16$	**$p < 0.0001$ ***
Female, n (%)	37 (0.544)	42 (0.553)	$\chi^2 = 0.008$	$p = 0.926$
Education, yr	14.6 ± 2.17	15.3 ± 2.53	$t = -1.68$	$p = 0.09$
Genotype (C/C: C/T, T/T)	32:35	22:53	$\chi^2 = 5.09$	**$p = 0.02$ ***
Age of onset, yr	18.3 ± 5.77	-	-	-
Illness duration, yr	14.2 ± 8.62	-	-	-
Total number of episodes	36.9 ± 45	-	-	-
Number of depressive episodes	14.7 ± 16.5	-	-	-
Number of manic episodes	7.8 ± 16.3	-	-	-
Number of hypomanic episodes	11.9 ± 18.3	-	-	-
Number of mixed episodes	2.2 ± 5.2	-	-	-
MADRS	4.7 ± 4.2	1 ± 1.9	$t = 6.56$	**$p < 0.0001$ ***
YMRS	1.7 ± 2.2	0.3 ± 0.8	$t = 4.88$	**$p < 0.0001$ ***
FAST total score	23.5 ± 13.9	7.1 ± 7.2	$t = 8.45$	**$p < 0.0001$ ***

3.2 Power Analysis

The power analysis results for the hypothesized regions indicated that power for the models ranged from 0.06 to 0.89, with the lowest power occurring in the left AIC and the highest power estimate in the left primary motor cortex. The power analysis results for the exploratory models indicated that, after correction, the power of the models ranged from 0.001 to 0.53. The highest power occurred in the cortical regions that reached significance. The average statistical power was estimated to be 0.03 in the non-significant regions. Statistical power tended to be higher in the right hemisphere than the left (mean(right) = 0.08, mean(left) = 0.03).

3.3 Allele Frequency

The *NRG1* genotypes met the criteria for Hardy Weinberg allele frequency distribution for the bipolar disorder group ($\chi^2 = 0.57$, $p = 0.75$), the healthy control group ($\chi^2 = 0.45$, $p = 0.80$), and the whole sample ($\chi^2 = 0.60$, $p = 0.74$). The genotype frequencies for the entire sample were C/C 54, C/T 72, and T/T 16 (**Table 3**). The frequency of the T/T genotype individuals was lower than that of the other genotypes in both the bipolar disorder group and healthy controls.

Table 3. Genotype frequencies of *NRG1* SNP rs6994992 for bipolar disorder participants and healthy controls

Table summarizing the number of participants in the bipolar disorder and healthy control groups with each genotype. The first three columns indicate the frequency of each genotype, with the total percentage of each genotype reported in the last row. The fourth column reports the number of participants in the combined T allele group, representing both the C/T and T/T genotypes.

	C/C	**C/T**	**T/T**	**C/T, T/T**
Bipolar Disorder	32	31	4	35
Healthy Controls	22	41	12	53
	38%	50.7%	11.3%	62%

A dominant model was used to compare genotype frequencies between each group, with the T allele carriers assessed together to improve statistical power (C/C vs. C/T, T/T). The results of a Chi-square analysis comparing the number of participants with and without the T allele between bipolar disorder and healthy control subjects indicates that the rs6994992 C/C genotype frequency is higher in bipolar disorder participants than in healthy controls ($\chi^2 = 5.02$, $p < 0.05$). Since allele frequency was shown to be different between groups, rs6994992 genotype was included as a variable in all analyses predicting ICM. The allelic discrimination plot showing the separation of alleles is included in **Figure 1**.

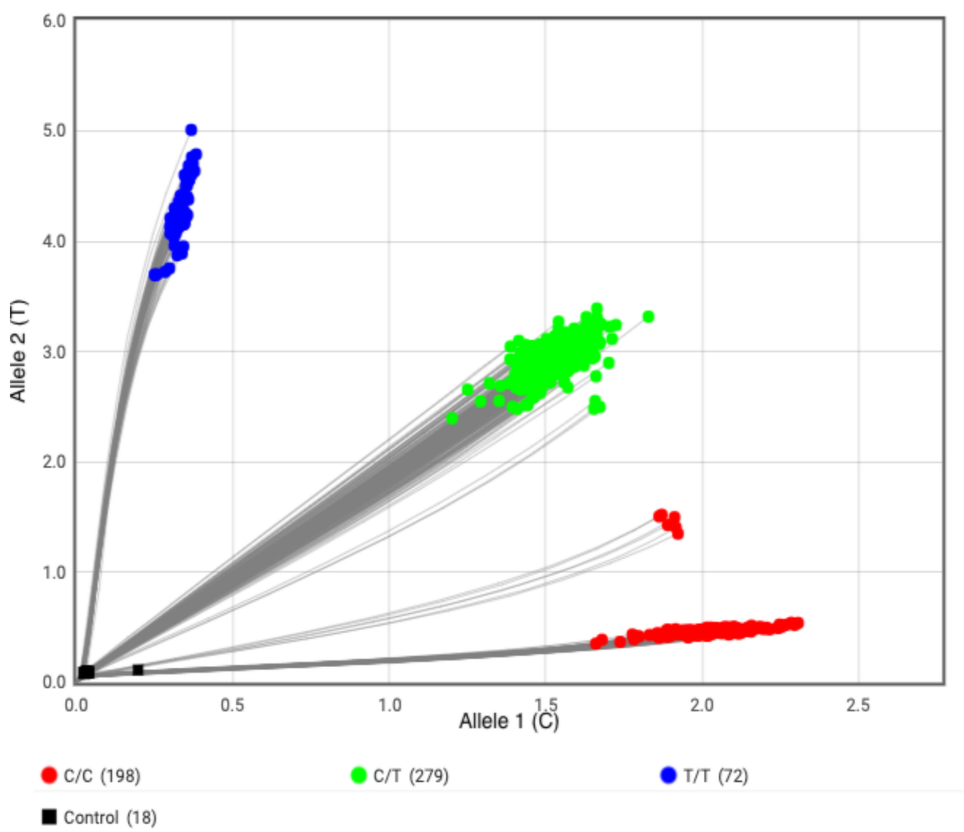

Figure 1. Allelic discrimination plot of rs6994992 genotype for all participants

This plot shows the separation of alleles for the entire participant sample. The y-axis represents the level of fluorescence corresponding to the T allele, while the x-axis represents that of the C allele. Points shown in blue represent individuals that are homozygous for the risk allele (T/T). Points in green represent those that are heterozygous (C/T). Points in red represent homozygous participants for the common allele (C/C). Points in black are control samples containing no template DNA for comparison. Bipolar disorder and healthy control participants are combined in this figure.

3.4 Primary Analysis - genotype, age, and diagnosis as predictors of ICM in the cortical regions of the salience network

3.4.1 Results in the dorsal anterior cingulate cortex (dACC)

Multiple linear regressions were performed to assess whether age, genotype and diagnosis can predict variation in R_1, a proxy measure of ICM, across participants. The regression results showed that these variables did not significantly predict ICM in the left dACC ($R^2 = 0.005$, $p = 0.29$) or right dACC ($R^2 = 0.016$, $p = 0.16$). Age was a significant predictor of ICM in the right dACC ($p < 0.05$, $\eta_p^2 = 0.029$), but no other predictive terms were significant in these models. The model assessing ICM in the left dACC did not meet the assumption of normally distributed residuals, and the model assessing the right dACC had significant autocorrelations. Additional linear regressions were conducted for each region, including an interaction term between diagnosis and genotype (diagnosis*genotype) to determine the moderating impact of genotype in the relationship between diagnosis and ICM. The models with and without the interaction term were compared through an ANOVA, and results indicate that genotype is not a significant moderator of the relationship between ICM and diagnosis in the left dACC (p = 0.97) or right dACC (p = 0.37).

Figure 2 shows the trajectory of R_1 signal intensity, used as a proxy measure of ICM, across the lifetime, comparing T allele carriers (C/T, T/T) to non-T-allele carriers (C/C), with bipolar disorder and healthy control subjects represented separately. Although genotype and diagnosis were not significant predictors of ICM within the linear models, the scatter plot indicates a trend that the age trajectory of R_1, a proxy measure of ICM, is blunted in individuals with bipolar disorder and a C/C genotype compared to healthy controls. The trajectory of individuals carrying a T allele is comparable between groups. This trend is observed in the left dACC (**Figure 2A**) and right dACC (**Figure 2B**). However, as mentioned previously, within the model assessing ICM, the diagnosis*genotype interaction term was not a significant predictor of ICM. Thus, this trend was not confirmed by our models.

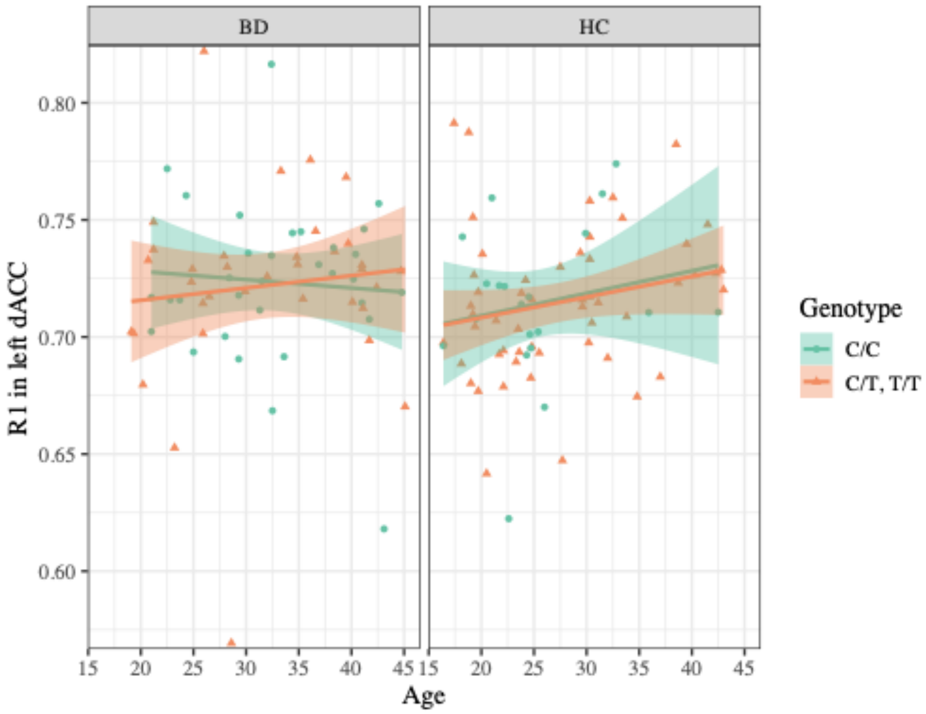
BD
HC
R1 in left dACC
0.80
0.75
0.70
0.65
0.60
15
20
25
30
35
40
45
Age
Genotype
C/C
C/T, T/T

A

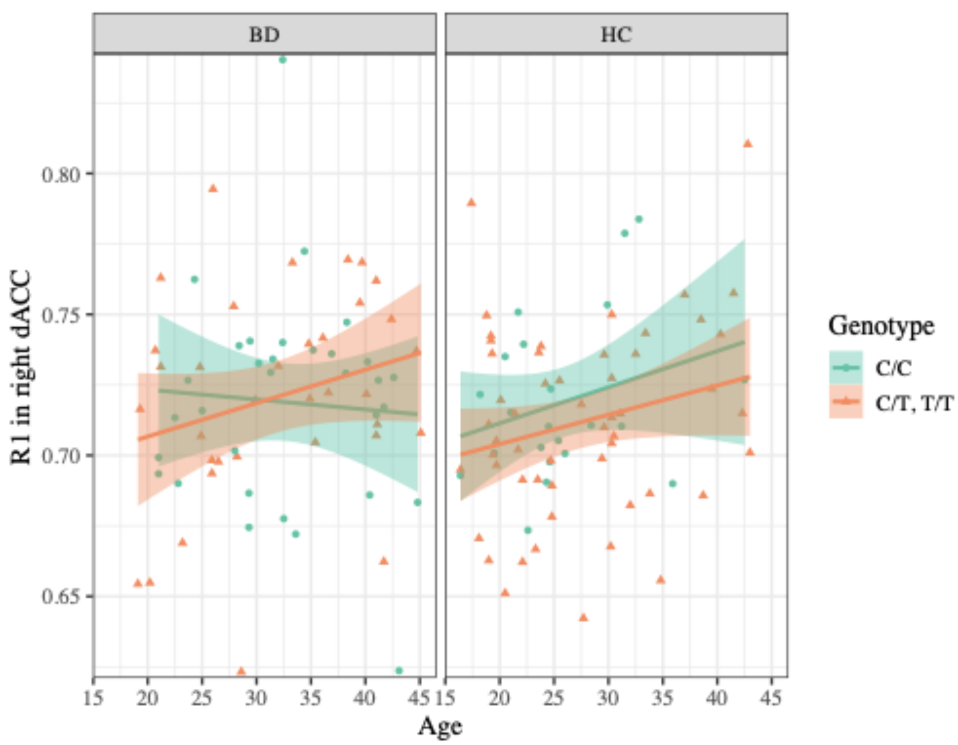
BD
HC
R1 in right dACC
0.80
0.75
0.70
0.65
15
20
25
30
35
40
45
Age
Genotype
C/C
C/T, T/T

B

Figure 2. Scatter plots representing R_1 signal intensity, a proxy measure of ICM, in the dorsal anterior cingulate cortex (dACC) as a function of age with comparisons of genotype and participant group

Figure **2A** shows the age trajectory of R_1 in the left dACC, while Figure **2B** shows the trajectory of R_1 in the right dACC. The left panel shows subjects with bipolar disorder, while the right panel shows healthy control subjects. Orange triangles indicate individual subjects with a C/T or T/T genotype, and green circles indicate individuals with a C/C genotype. Linear regression lines are fitted to the data and shading around the line represents confidence intervals.

3.4.2 Results in the anterior insular cortex (AIC)

The same linear regressions were performed using age, diagnosis, and genotype as predictor variables of ICM in the anterior insular cortex (AIC), separated bilaterally. The analyses showed that these variables did not significantly predict ICM in the left AIC ($R^2 = 0.002$, $p = 0.36$) or right AIC ($R^2 = 0.02$, $p = 0.14$). None of the predictor terms reached significance. The left AIC linear regression did not meet the normality assumption, and autocorrelations were present in the right AIC. Additional regressions, which included an interaction term between diagnosis and genotype, were performed to assess whether *NRG1* genotype is a significant moderator in the relationship between bipolar disorder and ICM. The models with and without the interaction term were compared through an ANOVA. Results indicated that genotype is not a significant moderator in the left AIC ($p = 0.54$) and right AIC ($p = 0.32$).

Figure 3 shows the trajectory of the R_1 signal, used as a proxy measure of ICM, as a function of age, comparing C/T and T/T genotypes to C/C individuals. Bipolar disorder and healthy control subjects are represented separately. Similar to the trend observed for the dACC in Figure 2, in the AIC, the bipolar disorder subjects with the C/C genotype display an evident blunted age trajectory slope compared to healthy controls with the same genotype. These trends are observed for the left AIC (**Figure 3A**) and the right AIC (**Figure 3B**).

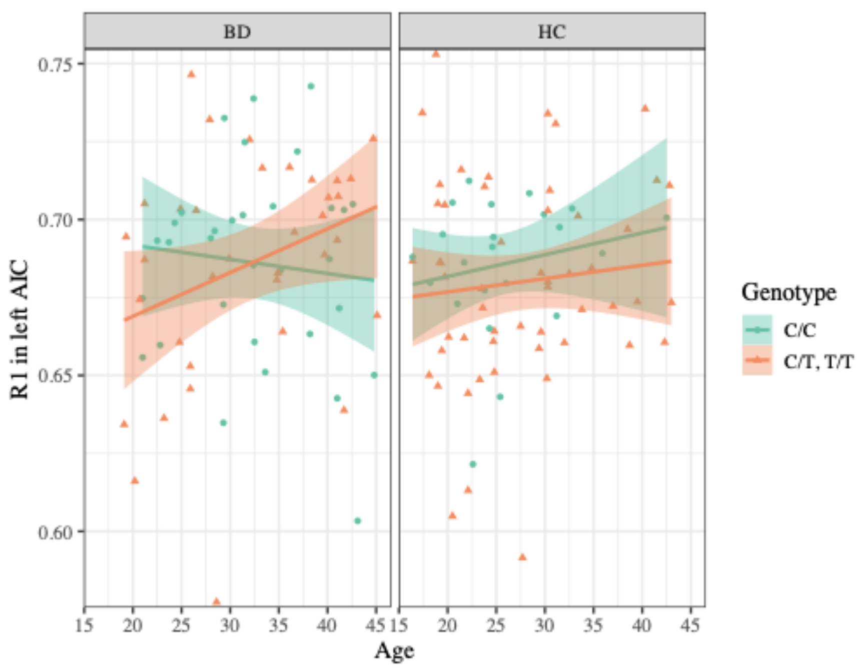

A

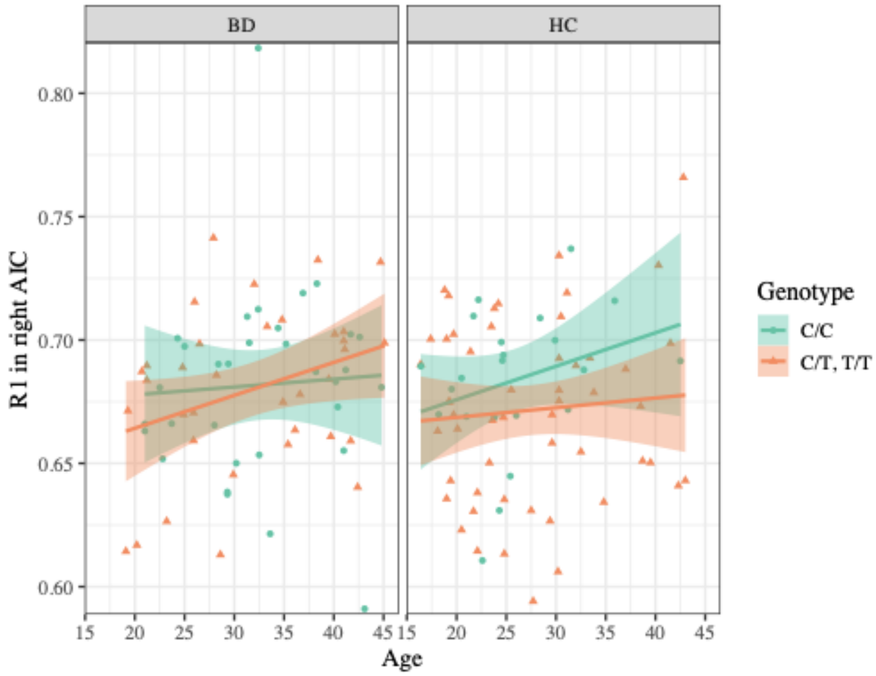

B

Figure 3. Scatter plot representing R_1 signal intensity, a proxy measure of ICM, in the anterior insular cortex (AIC) as a function of age with comparisons of genotype and participant group

Figure **3A** shows the age trajectory of R_1 in the left AIC, while Figure **3B** shows the trajectory of R_1 in the right AIC. The left panel shows subjects with bipolar disorder, while the right panel shows healthy control subjects. Orange triangles indicate individual subjects with a C/T or T/T genotype, and green circles indicate individuals with a C/C genotype. Linear regression lines are fitted to the data and shading around represents confidence intervals.

3.4.3 Results in the primary motor cortex

Additional linear regressions were performed with the same predictor variables for ICM in the bilateral primary motor cortex, which was meant to be a control region outside the salience network for comparison. The results of the analysis showed that the variables of age, diagnosis, and genotype together significantly predicted ICM in the left motor cortex ($R^2 = 0.09$, $p < 0.01$) and right motor cortex ($R^2 = 0.06$, $p < 0.05$). Age was a significant predictor of ICM in the left motor cortex ($p < 0.001$, $\eta_p^2 = 0.091$) and right motor cortex ($p < 0.05$, $\eta_p^2 = 0.043$). Both models did not meet the assumption of normal residuals, and significant autocorrelations were present in the model assessing ICM in the right motor cortex. Separate regressions were performed with an interaction term between diagnosis and genotype to assess whether *NRG1* genotype is a significant moderator in the relationship between bipolar disorder and ICM in the motor cortex. The models with and without the interaction term were compared through an ANOVA. The results of both analyses indicated that genotype is not a significant moderator in the left motor cortex ($p = 0.60$) and right motor cortex ($p = 0.63$).

Figure 4 shows the trajectory of the R_1 signal, used as a proxy measure of ICM, across the lifetime, comparing C/T and T/T genotypes to C/C individuals. Bipolar disorder and healthy control subjects are shown in separate plots. **Figure 4A** shows the results from the left motor cortex, while **Figure 4B** shows the results from the right motor cortex. As with the dACC and AIC, the ICM signal age trajectory in the motor cortex was blunted in bipolar disorder participants with C/C genotype. The age trajectory of subjects with C/T and T/T genotypes are comparable between bipolar disorder and healthy control groups.

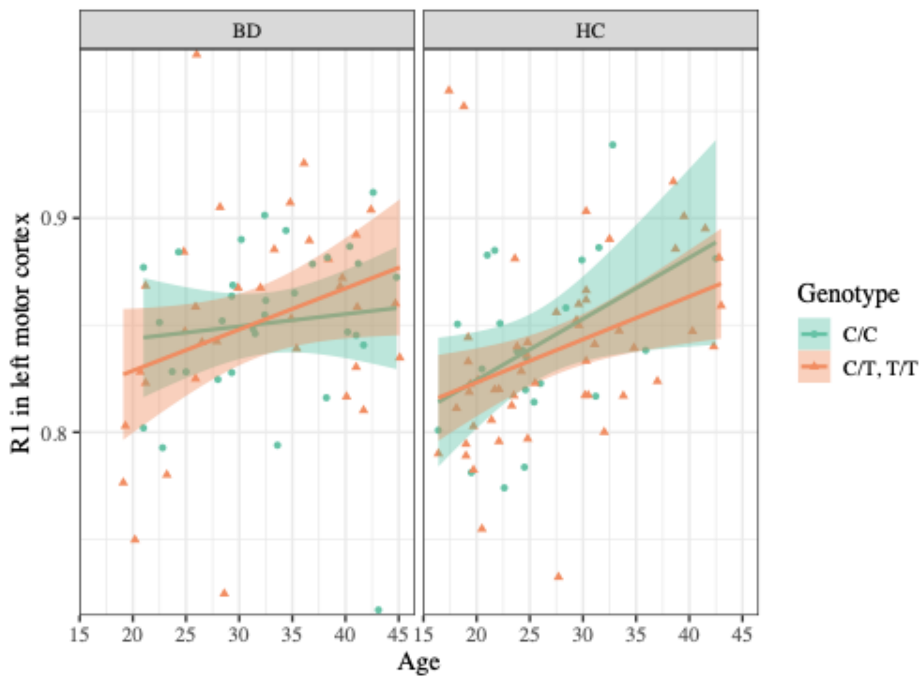

A

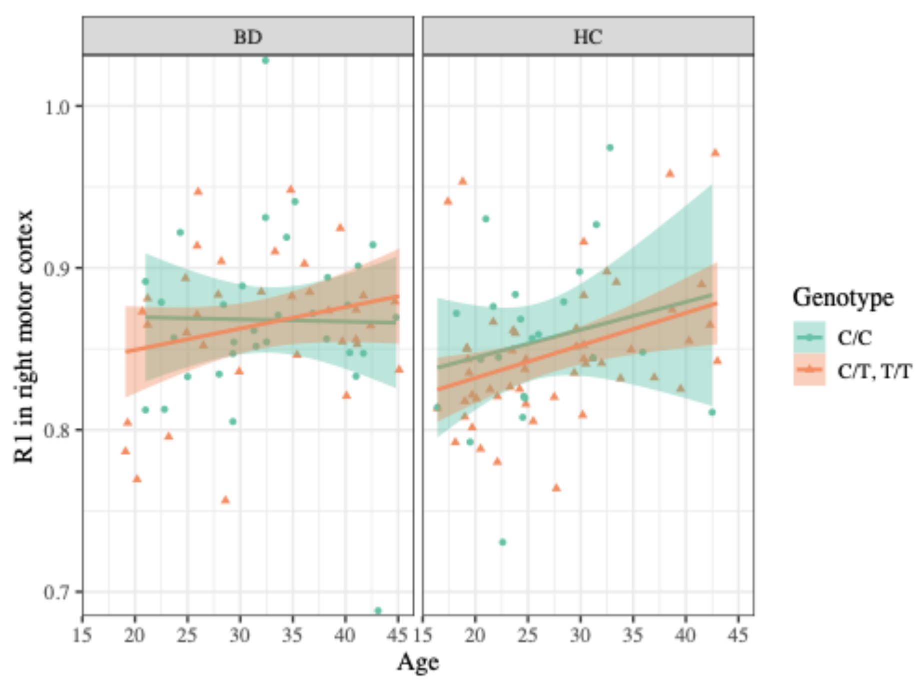

B

Figure 4. Scatter plot representing R_1 signal intensity, a proxy measure of ICM, in the primary motor cortex as a function of age with comparisons of genotype and participant group

Figure **4A** shows the age trajectory of R_1 in the left motor cortex, while Figure **4B** shows the trajectory of R_1 in the right motor cortex. The left panel shows subjects with bipolar disorder, while the right panel shows healthy control subjects. Orange triangles indicate individual subjects with a C/T or T/T genotype, and green circles indicate individuals with a C/C genotype. Linear regression lines are fitted to the data and shading around represents confidence intervals.

3.5 Exploratory Analysis - additional regions where ICM is predicted by age, diagnosis and genotype

Regions of interest from the MSMAll atlas were combined into 22 regions based on shared functional connectivity (Glasser et al., 2016). ICM signal from each ROI was averaged to form each of the 22 regions, assessed bilaterally, for a total of 44 analyzed regions. ROIs assessed in the previous hypothesis analysis (regions corresponding to the dACC, AIC, and primary motor cortex) were not assessed as part of this exploratory analysis. Linear regressions were performed separately for each region to identify cortical regions where ICM is predicted by age, diagnosis, and genotype. Corrections were applied for multiple comparisons. After correction, the normal significance threshold 0.05 became 0.00114 ($\alpha = 0.05/44$ tests) for model p values. The effect size of each predictive term was calculated as partial eta squared (η_p^2). Thirty-five models did not meet the assumption of normally distributed residuals, three did not meet the assumption of homoscedasticity, and thirty-one tested significant for autocorrelations. The results of all models are summarized in **Table 4.** After correction for multiple comparisons, it was found that ICM is significantly predicted by age, diagnosis and genotype in the right premotor cortex (R^2 = 0.095, $p < 0.001$) and the right inferior frontal cortex (IFC) (R^2 = 0.098, $p < 0.001$). Age was a significant predictor in five regions of the left hemisphere and eight regions of the right hemisphere, including the right premotor ($p < 0.001$) and inferior frontal cortices ($p < 0.01$). Effect sizes for each predictor term are reported in **Table 5**. Across all models, partial eta squared calculated for the age term ranged from 0.0012 to 0.086, with the lowest estimate in the left dorsal stream visual cortex and the highest in the right premotor cortex. For the diagnosis term, the effect size was lowest in the right early auditory cortex (η_p^2 = 0.0000004), and the largest effect size was found in the right lateral temporal cortex (η_p^2 = 0.027). Finally, the smallest effect size estimate for the genotype term was in the left orbital and polar frontal cortex (η_p^2 = 0.00002), and the largest was in the right ventral stream visual cortex (η_p^2 = 0.014).

Table 4. Results of exploratory analysis assessing the effect of diagnosis and genotype on ICM signal in the cerebral cortex

Table summarizing the results of linear regression models conducted separately for 44 parcellated regions of the cerebral cortex. The model p-value and adjusted R^2 are reported in addition to the p-values of the individual predictors (age, diagnosis and genotype). Results are reported separately for the regions of the left hemisphere and the right hemisphere. (**) indicates statistical significance at a level of p=0.00114 for models and (*) at a level of p=0.05 for individual predictors.

	Left Hemisphere					Right Hemisphere				
Section name	**Model p**	**Model adjusted R^2**	**Age p**	**Diagnosis p**	**Genotype p**	**Model p**	**Model adjusted R^2**	**Age p**	**Diagnosis p**	**Genotype p**
Primary Visual Cortex	0.1442	0.0174	0.0893	0.3625	0.9425	0.4613	-0.0029	0.1830	0.9350	0.4530
Early Visual Cortex	0.1031	0.0229	0.0657	0.3288	0.7053	0.2756	0.0064	0.1600	0.3850	0.1620
Dorsal Stream Visual Cortex	0.4014	-0.0003	0.6880	0.1550	0.9460	0.6929	-0.0111	0.3400	0.5570	0.4610
Ventral Stream Visual Cortex	0.1309	0.0190	0.1450	0.2120	0.9130	0.2211	0.0102	0.1160	0.5900	0.1610
MT+ Complex and Neighboring Visual Areas	0.2928	0.0054	0.2920	0.2430	0.9360	0.6090	-0.0083	0.2210	0.3650	0.7570
Somatosensory and Motor Cortex	0.3215	0.0037	0.1080	0.7190	0.9420	0.0882	0.0254	**0.0290***	0.6980	0.6590
Paracentral Lobular and Mid Cingulate Cortex	0.0122	0.0557	**0.0073***	0.5420	0.3782	0.0541	0.0331	**0.0177***	0.9431	0.3371
Premotor Cortex	0.0401	0.0377	**0.0077***	0.8886	0.7938	**0.0008****	0.0954	**0.0004***	0.4285	0.7750

Posterior Opercular Cortex	0.4727	-0.0034	0.1390	0.9900	0.9160	0.0813	0.0267	**0.0454***	0.4495	0.6489
Early Auditory Cortex	0.6124	-0.0085	0.5080	0.3760	0.8700	0.3198	0.0038	0.0805	0.9939	0.8555
Auditory Association Cortex	0.4384	-0.0019	0.1960	0.6120	0.9500	0.0298	0.0423	**0.0258***	0.2673	0.8479
Insular and Frontal Opercular Cortex	0.7647	-0.0133	0.6720	0.4870	0.7900	0.2720	0.0067	0.1120	0.8330	0.4560
Medial Temporal Cortex	0.6821	-0.0107	0.4000	0.7480	0.6120	0.1932	0.0125	0.1330	0.9920	0.1660
Lateral Temporal Cortex	0.3025	0.0048	0.3220	0.2600	0.7890	0.0385	0.0384	0.1846	0.0524	0.8644
Temporo-Parieto-Occipital Junction	0.0976	0.0238	0.0685	0.3003	0.8830	0.3262	0.0035	0.1130	0.9370	0.4380
Superior Parietal Cortex	0.0518	0.0338	0.0658	0.2080	0.7046	0.1368	0.0183	0.0682	0.7537	0.3338
Inferior Parietal Cortex	0.0586	0.0319	**0.0366***	0.3449	0.9256	0.2695	0.0068	0.1430	0.6460	0.4740
Posterior Cingulate Cortex	0.0551	0.0328	**0.0364***	0.4403	0.5012	0.1495	0.0168	0.1100	0.7430	0.2140
Anterior Cingulate and Medial Prefrontal Cortex	0.4644	-0.0030	0.4620	0.2930	0.9030	0.2609	0.0074	0.1010	0.8300	0.4920
Orbital and Polar Frontal Cortex	0.5413	-0.0060	0.1610	0.9410	0.9550	0.0134	0.0543	**0.0033***	0.8215	0.6058
Inferior Frontal Cortex	0.2573	0.0076	0.0538	0.8155	0.7107	**0.0006****	0.0984	**0.0011***	0.1667	0.8892
Dorsolateral Prefrontal Cortex	0.1448	0.0173	**0.0301***	0.9577	0.8612	0.0367	0.0391	**0.0112***	0.6228	0.9242

Table 5. Effect sizes of predictor variables in exploratory models separated by hemisphere

Table summarizing the effect size of age, diagnosis and genotype as predictive variables of ICM content in 22 regions of the cerebral cortex, reported separately for left and right hemispheres. Effect size is reported as partial eta squared (η_p^2).

	Left Hemisphere			Right Hemisphere		
Section name	**η_p^2 (age)**	**η_p^2 (diagnosis)**	**η_p^2 (genotype)**	**η_p^2 (age)**	**η_p^2 (diagnosis)**	**η_p^2 (genotype)**
Primary Visual Cortex	0.0208	0.0060	0.00004	0.0128	0.00005	0.0041
Early Visual Cortex	0.0243	0.0069	0.00104	0.0142	0.0055	0.0141
Dorsal Stream Visual Cortex	0.0012	0.0146	0.00003	0.0066	0.0025	0.00394
Ventral Stream Visual Cortex	0.0153	0.0113	0.00009	0.0178	0.0021	0.0142
MT+ Complex and Neighboring Visual Areas	0.0080	0.0099	0.00005	0.0109	0.0060	0.0007
Somatosensory and Motor Cortex	0.0186	0.0009	0.00004	0.0341	0.0011	0.00142
Paracentral Lobular and Mid Cingulate Cortex	0.0511	0.0027	0.00563	0.0401	0.00004	0.00668
Premotor Cortex	0.0503	0.0001	0.0005	0.0864	0.0045	0.00059
Posterior Opercular Cortex	0.0158	0.000001	0.00008	0.0287	0.0042	0.00151
Early Auditory Cortex	0.0032	0.0057	0.00019	0.0220	0.0000004	0.00024
Auditory Association Cortex	0.0121	0.0019	0.00003	0.0355	0.0089	0.00027
Insular and Frontal Opercular Cortex	0.0013	0.0035	0.00052	0.0182	0.0003	0.00403
Medial Temporal Cortex	0.0051	0.0007	0.00187	0.0163	0.000001	0.01383
Lateral Temporal Cortex	0.0071	0.0092	0.00052	0.0127	0.0270	0.00021
Temporo-Parieto-Occipital Junction	0.0238	0.0078	0.00016	0.0181	0.00005	0.00436
Superior Parietal Cortex	0.0243	0.0115	0.00104	0.0239	0.0007	0.00677
Inferior Parietal Cortex	0.0313	0.0065	0.00006	0.0155	0.0015	0.00372
Posterior Cingulate Cortex	0.0313	0.0043	0.00328	0.0184	0.0008	0.01119

Anterior Cingulate and Medial Prefrontal Cortex	0.0039	0.0080	0.00011	0.0194	0.0003	0.00343
Orbital and Polar Frontal Cortex	0.0142	0.00004	0.00002	0.0608	0.0004	0.00194
Inferior Frontal Cortex	0.0267	0.0004	0.001	0.0744	0.0138	0.00014
Dorsolateral Prefrontal Cortex	0.0336	0.00002	0.00022	0.0457	0.0018	0.00007

CHAPTER 4 - DISCUSSION AND CONCLUSIONS

4.1 Summary of Results

A cross-sectional assessment of intracortical myelin content was conducted in individuals with bipolar disorder type I to identify the impacts of age, diagnosis and *NRG1* rs6994992 genotype on ICM content. An initial *a priori* analysis was conducted to determine whether R_1, a proxy measure of ICM, could be significantly predicted by age, diagnosis, and genotype in the cortical regions of the salience network, the dorsal anterior cingulate cortex (dACC) and the anterior insular cortex (AIC). A control region, the primary motor cortex, was also included for comparison. This analysis indicated that the primary motor cortex was the only region significantly predicted by age, diagnosis, and genotype. However, ICM in the bilateral primary motor cortex and the right dACC was significantly predicted by participant age alone, with medium effect sizes in the left motor cortex ($\eta_p^2 = 0.091$) and right motor cortex ($\eta_p^2 = 0.043$). These models were compared to models that included an interaction term between diagnosis and genotype to assess whether genotype was a significant moderator of ICM in our regions of interest. These analyses suggested that rs6994992 genotype is not a significant moderator of ICM in these specific regions. A secondary exploratory analysis was conducted to identify if R_1, and thus ICM, in any other regions of the cerebral cortex, was significantly predicted by age, diagnosis, and genotype. This analysis significantly predicted ICM content in the right premotor and inferior frontal cortices (IFC). Age was a significant predictor within these regions, but diagnosis and genotype were not.

4.2 The impact of age on ICM

Age as a significant predictor of ICM coincides with previous research regarding ICM and confirms our prediction that age impacts ICM content across cortical regions. Our results found that age significantly predicted ICM in the right dACC, bilateral motor cortex, right premotor cortex, and right IFC. The exploratory analysis additionally identified five regions in the left hemisphere and eight in the right where age was a significant predictor. These regions can be found in **Table 4**.

Grydeland and colleagues (2013) identified that cortical myelin follows an inverted-U-shaped trajectory over the lifetime in healthy individuals. The cingulate and insular cortices were two of the most affected regions identified in this study and showed greater effects in the right hemisphere than the left (Grydeland et al., 2013). The impact of age on ICM in the ACC has been replicated by our group, finding that ICM in the ACC follows the typical inverted-U trajectory but that this trajectory is blunted in individuals with bipolar disorder (Sehmbi et al., 2019). Although past studies have found a large effect of age on ICM in the ACC, our study only found a significant prediction of age in the right dACC, with a small effect size ($\eta_p^2 = 0.029$). Additionally, although the same inverted-U trajectory of cortical myelination has been found in the insular cortex in the past (Grydeland et al., 2013), our assessment of ICM in the AIC was not significant. The age predictor within these models also did not reach significance but neared significance in the right AIC ($p = 0.07$). Our models show larger effect sizes in the right hemisphere of the dACC and AIC compared to the left hemisphere, which aligns with past research assessing cortical myelin in these regions (Grydeland et al., 2013).

The blunted age trajectory of ICM in bipolar disorder has been identified across cortical regions, including the ACC, but was found to have the largest impact in the bilateral premotor and primary motor cortices with effect size estimates of 0.1 (Sehmbi et al., 2019). The results of the current experiment replicate the large effect sizes of age on ICM in the premotor and primary motor cortices. Age as a predictor of ICM within our models had the largest effect size in the primary motor cortex ($\eta_p^2 = 0.091$), followed by the premotor cortex ($\eta_p^2 = 0.086$).

Myelin content within the cerebral cortex is higher in primary sensory and motor regions, notably the primary motor cortex, and lower in association areas, including the cingulate and insular cortices (Glasser & Van Essen, 2011). Thus, the large magnitude of ICM deficits in motor regions may result from more myelin within these cortical regions. Similarly, small magnitudes of age-related ICM effects in the dACC and lack of association in the AIC may be due to a lower myelin content within these regions. Our models of the AIC had small effect sizes of the age predictor in the left ($\eta_p^2 = 0.017$) and right ($\eta_p^2 = 0.024$) insula. These small effect sizes corresponded to low statistical power in these regions, with the AIC having a power of 0.06-0.23 and the dACC having a power of 0.1-0.2. Low statistical power in this region likely prevented the age term from reaching significance in these lightly myelinated regions where the effect of age on ICM is less than in primary motor regions.

From the exploratory analysis, the right inferior frontal cortex (IFC) and right premotor cortex were the only regions where ICM was significantly predicted by age, diagnosis and genotype, and age alone being a significant predictor. The significance and large effect size of the premotor cortex ($\eta_p^2 = 0.086$) align with the results of the primary motor cortex and with past research identifying these two regions as having the largest impact of age on ICM in the cortex (Sehmbi et al., 2019). However, the effect size of the age predictor in the IFC was comparable to that of the premotor cortex ($\eta_p^2 = 0.074$) and one of the largest among cortical regions. This is surprising given that the IFC has not previously been isolated as a region of interest for age-related ICM deficits. The IFC is primarily responsible for speech production and language processing, with additional roles in working memory and executive functioning (Baldo & Dronkers, 2006). Specifically, the right IFC controls executive functioning during tasks through inhibitory control mechanisms. Lesions in this region lead to impairments in executive functioning during response inhibition tasks (Aron et al., 2003). The IFC has been identified as being altered in individuals with bipolar disorder, contributing to cognitive deficits associated with the disorder. Even individuals in euthymia show executive functioning task-related decreases in activation in the IFC compared to healthy controls (Townsend et al., 2012). Additionally, in individuals with bipolar disorder, a greater duration of illness has been associated with decreased grey matter volume in the right IFC (Hajek et al., 2013).

Interestingly, the IFC, compared to other cortical regions, has moderate thickness but is lightly myelinated within the cortex (Glasser et al., 2016). The myelinated fibres within this region are localized at the white matter boundary, creating light ICM within the IFC. Additionally, the grey/white matter contrast, an early measure of myelin content, decreases longitudinally in the IFC (Salat et al., 2009; Vidal-Piñeiro et al., 2016). Despite light myelination in this region, our study found that ICM in the IFC is significantly predicted by age, diagnosis and genotype, and particularly age is a significant predictor of ICM. The large effect size in this region ($\eta_p^2 = 0.074$) contrasts other lightly myelinated regions that we studied, including the dACC and insula. This significant age effect highlights the IFC as a region of particular interest for future studies on ICM deficits.

Interestingly, the three regions where we found the largest effect of age on ICM - the right premotor cortex, bilateral primary motor cortex, and right inferior frontal cortex - are all involved in motor control. The right IFC controls the premotor cortex through its role in response inhibition, selecting appropriate voluntary movements for the primary motor cortex to initiate. fMRI studies have shown that the right IFC initiates stopping using beta-band oscillations on the premotor cortex (Schaum et al., 2021). These two regions have also been shown to be structurally connected using diffusion tractography (Swann et al., 2012). Our results reveal the potential role of ICM and age for motor inhibitory control in the IFC and primary and premotor cortices.

4.3 The impact of bipolar disorder diagnosis on ICM

Although the diagnosis term was not a significant individual predictor of ICM in any cortical regions studied, the models including diagnosis as predictors were significant in the bilateral motor cortex, premotor cortex, and inferior frontal cortex. Past studies have identified motor dysfunction, particularly impairments in fine motor control, in individuals with bipolar disorder (Negash et al., 2004). Additionally, motor speed dysfunction has been identified in both individuals with bipolar disorder who are euthymic and their unaffected relatives, suggesting motor impairments as a possible endophenotype of the disorder (Correa-Ghisays et al., 2017). The significant models, including diagnosis in the motor regions of the cortex, align with what is known about deficits of fine motor functioning in bipolar disorder. The premotor, primary motor and inferior frontal cortices are involved in motor inhibitory control, and deficits in these areas may contribute to deficits in motor function found in the disorder.

4.4 The impact of NRG1 genotype on ICM

One research aim of this study was to identify whether *NRG1* genetic variation moderates the relationship between bipolar disorder and ICM in the salience network. We found that rs6994992 genotype alone is not a significant moderator of this relationship nor a significant predictor of ICM content in any cortical regions studied. In the exploratory analysis, the largest effect size of the genotype predictor in the models was 0.01 in various regions of the right hemisphere. These minor effects of the SNP genotype contribute to low statistical power within the models and lower the possibility of identifying a significant effect of the genotype predictor variable. Genotype studies generally have large sample sizes to compensate for the small effect sizes of individual SNPs and provide sufficient statistical power. Alternative methods have also been developed to overcome the low statistical power of small sample sizes, including calculating polygenic risk scores of multiple *a priori* SNPs.

As mentioned previously, bipolar disorder is a polygenic disorder with many genetic factors contributing to the heritability of the disorder. Polymorphisms are only one of these factors, where the combined impact of known risk SNPs is estimated to contribute 8% of the heritability of the disorder (Gordovez & McMahon, 2020; Stahl et al., 2019). Thus, individual SNPs contribute small effect sizes to the risk of developing bipolar disorder. Findings from past studies assessing structural brain changes associated with rs6994992 in bipolar disorder are conflicting, with some studies finding a significant impact of the SNP and others not. The results of the current experiment confirm the heterogeneity of these studies, having been unable to find a significant association of the SNP with ICM. These conflicting results are also observed for structural brain changes in bipolar disorder, with some large-scale meta-analyses unable to significantly conclude a direction of effect due to the heterogeneity between bipolar disorder samples across studies (Hajek et al., 2005). Of the studies that have assessed the impact of *NRG1* risk variants on brain structural changes, few have found a significant association with bipolar disorder. Of those that find an association, it has been shown that the magnitude of effect in bipolar disorder is less than in schizophrenia (Chong et al., 2008). Although *NRG1*

SNPs have been established as risk factors for schizophrenia, the magnitude of influence is not as large in bipolar disorder as in schizophrenia. Other studies that found an association with bipolar disorder included participants with symptoms of psychosis (Cao et al., 2014). Psychotic symptoms have been established as a significant risk factor associated with rs6994992 genotype, and the impact of psychotic symptoms may drive the significant associations found between bipolar disorder and rs6994992 genotype (Green et al., 2005).

For the hypothesis-driven analysis, we chose *a priori* to focus on ICM in the dACC and AIC because past research indicates these areas are related to *NRG1* genotype and structural brain changes. The ACC has been identified as a region with significant white matter alterations in healthy individuals and those with various psychiatric disorders associated with *NRG1* genetic variation. One study by Barnes and colleagues found that grey matter volume is significantly decreased in the ACC in healthy individuals carrying an rs6994992 T allele (Barnes et al., 2012). Another study by Wang and colleagues found that white matter integrity in the ACC is significantly reduced in individuals with schizophrenia with the rs6994992 T allele (Wang et al., 2009). From these results, it is unlikely that bipolar disorder is the factor driving our differing results. Instead, it seems that intracortical myelin may be affected by rs6994992 genotype differently than white matter, contributing to variable results.

In addition to testing the statistical significance and effect size for predictors of ICM, scatter plots were created to visualize trends in the data set for future research. Through this, it is evident that although *NRG1* genotype was not a significant predictor of ICM in our models, the age-related ICM trajectory is altered between genotype groups in individuals with bipolar disorder. Participants with a C/C genotype have a blunted age trajectory compared to those carrying a T allele (C/T and T/T genotypes). This pattern is unexpected given that most past research has identified the T allele as a risk factor for structural deficits in the cerebral cortex. However, one study of rs6994992 in bipolar disorder also identified the C allele as a risk factor. In this study, Prata and colleagues found that the C allele of rs6994992 was associated with mood-incongruent psychotic features in bipolar disorder (Prata et al., 2009).

Our study found that the frequency of C/C genotypes was significantly higher in BD than in HC. This indicates that the C/C genotype may be a potential risk factor for bipolar disorder, in which more individuals with the diagnosis have the C/C genotype, and those with the genotype have a hindered age-related trajectory of ICM across cortical regions. Brain structural changes have not previously been associated with the C/C genotype in bipolar disorder, and thus, no comparisons can be made to our results. However, we highlight that the C/C genotype may impact ICM in individuals with bipolar disorder.

4.5 Limitations and Strengths

Our results should be interpreted in light of the following limitations. Our sample consisted of 67 bipolar disorder participants and 75 healthy controls. While this sample size is typical for imaging studies, it contributes to low statistical power for the genotype term, which generally had low effect sizes (range 0.00002-0.01). A larger sample size, comparable to other genetic studies, may have allowed the *NRG1* genotype term to reach significance.

Additionally, because of the relative rarity of the T/T genotype, only four participants in our bipolar disorder group had this genotype. Because of this, and to maximize statistical power, all individuals carrying a T allele (genotypes C/T and T/T) were combined into one group, similar to past studies of rs6994992 (Barnes et al., 2012; Wang et al., 2009). While this benefitted our statistical power, it prevented us from making conclusions about the nature of allelic separation in our results, and we were unable to determine whether the effects of genotype are dominant or codominant in our sample.

Another important limitation to note is that most of our models did not meet the required assumptions of a linear model. Four of the six models in the hypothesized analysis did not have normally distributed residuals, and three had significant autocorrelations. From the exploratory analysis, thirty-five of forty-four models did not have normally distributed residuals, three had an unequal variance of residuals, and thirty-one had significant autocorrelations. The findings of this study should be interpreted with caution due to these violated assumptions. Future work will focus on finding alternative statistical tests that better fit the data of this study.

Despite these limitations, this study serves as the first assessment of genetic risk factors of intracortical myelination using a T_1w approach in bipolar disorder type I. Our findings serve as a basis for important research identifying the role of genetics for ICM in bipolar disorder. Specifically, we have identified a region not previously associated with ICM in bipolar disorder, the right inferior frontal cortex, which should be further investigated.

4.6 Implications for Future Research

Future studies should extend our findings by addressing the potential role of intracortical myelination in inhibitory motor control, specifically in the right inferior frontal cortex. Given that impairment of fine motor control is a symptom observed in some individuals with bipolar disorder (Negash et al., 2004), the inferior frontal cortex and the highly myelinated premotor and primary motor cortices are of interest for assessing ICM deficits in bipolar disorder. Additionally, since we found a significant association between age and ICM in the inferior frontal cortex with moderate effect size, future studies should identify whether the blunted inverted-U trajectory of ICM across age in bipolar disorder is replicated in this region.

Although our study did not find a significant prediction of *NRG1* genotype on ICM, future studies should continue this area of research by assessing the combined impact of multiple known bipolar disorder risk polymorphisms. This can be done using a polygenic risk score method. In contrast to a candidate gene approach, calculating polygenic risk scores involves identifying SNPs already known to be associated with bipolar disorder and weighting them according to their relative effect size. This provides the benefit of increasing statistical power even in smaller sample sizes and improves the possibility of finding a significant effect. Concerning intracortical myelin, multiple genes are known to be involved in the process of cortical myelination while also conferring risk to bipolar disorder. Many of these genes are involved in different areas of the same signalling cascades. Future studies assessing ICM deficits in bipolar disorder should combine *NRG1* SNPs with others involved in oligodendrocyte development, weighted into a polygenic risk score, to improve the predictive capabilities of the SNPs.

Our study visually observed a trend in our dataset in which bipolar disorder participants with a C/C genotype had a blunted ICM age-related trajectory compared to healthy control participants. Future studies should identify the potential susceptibility role of the *NRG1* C/C genotype for ICM deficits in bipolar disorder. These trends should be quantitatively tested to determine the magnitude of change in ICM between these groups.

4.7 Conclusions

Our study found that ICM is predicted by age, bipolar disorder diagnosis, and *NRG1* rs6994992 genotype in the bilateral primary motor cortex, the right premotor cortex, and the right inferior frontal cortex. Age is a significant predictor of ICM in the previously mentioned regions in addition to the right dorsal anterior cingulate cortex. ICM was not significantly predicted by bipolar diagnosis and *NRG1* genotype alone. In a visual assessment of age-related trajectories of ICM, we observed that bipolar disorder individuals with a C/C genotype have a blunted slope of their age trajectory compared to healthy controls with the same genotype. Our findings identify the C/C genotype as a potential susceptibility factor for ICM deficits in bipolar disorder. We also identify the right inferior frontal cortex as a region where age significantly impacts ICM. Future research should extend our findings by assessing the role of ICM in inhibitory motor control in bipolar disorder, specifically in the right inferior frontal cortex. Additionally, future research is needed to quantitatively assess whether ICM deficits occur in individuals with bipolar disorder and a C/C genotype of the *NRG1* rs6994992 polymorphism.

CHAPTER 5 - REFERENCES

Altshuler, L., Bookheimer, S., Townsend, J., Proenza, M. A., Sabb, F., Mintz, J., & Cohen, M. S. (2008). Regional brain changes in bipolar I depression: A functional magnetic resonance imaging study. *Bipolar Disorders*, *10*(6), 708–717. https://doi.org/10.1111/j.1399-5618.2008.00617.x

American Psychiatric Association. (2013). *Diagnostic and statistical manual of mental disorders* (5th ed.). https://dsm.psychiatryonline.org/doi/book/10.1176/appi.books.9780890425596

Aron, A. R., Fletcher, P. C., Bullmore, E. T., Sahakian, B. J., & Robbins, T. W. (2003). Stop-signal inhibition disrupted by damage to right inferior frontal gyrus in humans. *Nature Neuroscience*, *6*(2), Article 2. https://doi.org/10.1038/nn1003

Bakker, S. C., Hoogendoorn, M. L. C., Selten, J. P., Verduijn, W., Pearson, P. L., Sinke, R. J., & Kahn, R. S. (2004). Neuregulin 1: Genetic support for schizophrenia subtypes. *Molecular Psychiatry*, *9*(12), 1061–1063.

Baldessarini, R. J., Bolzani, L., Cruz, N., Jones, P. B., Lai, M., Lepri, B., Perez, J., Salvatore, P., Tohen, M., Tondo, L., & Vieta, E. (2010). Onset-age of bipolar disorders at six international sites. *Journal of Affective Disorders*, *121*(1), 143–146. https://doi.org/10.1016/j.jad.2009.05.030

Baldo, J. V., & Dronkers, N. F. (2006). The role of inferior parietal and inferior frontal cortex in working memory. *Neuropsychology*, *20*(5), 529–538. https://doi.org/10.1037/0894-4105.20.5.529

Barnes, A., Isohanni, M., Barnett, J. H., Pietiläinen, O., Veijola, J., Miettunen, J., Paunio, T., Tanskanen, P., Ridler, K., & Suckling, J. (2012). Neuregulin-1 genotype is associated with structural differences in the normal human brain. *Neuroimage*, *59*(3), 2057–2061.

Bartzokis, G., Beckson, M., Lu, P. H., Nuechterlein, K. H., Edwards, N., & Mintz, J. (2001). Age-Related Changes in Frontal and Temporal Lobe Volumes in Men: A Magnetic Resonance Imaging Study. *Archives of General Psychiatry*, *58*(5), 461–465. https://doi.org/10.1001/archpsyc.58.5.461

Bartzokis, G., Lu, P. H., Raven, E. P., Amar, C. P., Detore, N. R., Couvrette, A. J., Mintz, J., Ventura, J., Casaus, L. R., Luo, J. S., Subotnik, K. L., & Nuechterlein, K. H. (2012). Impact on intracortical myelination trajectory of long acting injection versus oral risperidone in first-episode schizophrenia. *Schizophrenia Research*, *140*(1), 122–128. https://doi.org/10.1016/j.schres.2012.06.036

Bartzokis, G., Lu, P. H., Stewart, S. B., Oluwadara, B., Lucas, A. J., Pantages, J., Pratt, E., Sherin, J. E., Altshuler, L. L., Mintz, J., Gitlin, M. J., Subotnik, K. L., & Nuechterlein, K. H. (2009). In vivo evidence of differential impact of typical and atypical antipsychotics on intracortical myelin in adults with schizophrenia. *Schizophrenia Research*, *113*(2), 322–331. https://doi.org/10.1016/j.schres.2009.06.014

Bartzokis, G., Mintz, J., Marx, P., Osborn, D., Gutkind, D., Chiang, F., Phelan, C. K., & Marder, S. R. (1993). Reliability of in vivo volume measures of hippocampus and other brain structures using MRI. *Magnetic Resonance Imaging*, *11*(7), 993–1006. https://doi.org/10.1016/0730-725X(93)90218-3

Bellani, M., Boschello, F., Delvecchio, G., Dusi, N., Altamura, C. A., Ruggeri, M., &

Brambilla, P. (2016). DTI and Myelin Plasticity in Bipolar Disorder: Integrating Neuroimaging and Neuropathological Findings. *Frontiers in Psychiatry*, *7*. https://www.frontiersin.org/articles/10.3389/fpsyt.2016.00021

Bennett, M. R. (2011). Schizophrenia: Susceptibility genes, dendritic-spine pathology and gray matter loss. *Progress in Neurobiology*, *95*(3), 275–300.

Blumberg, H. P., Stern, E., Martinez, D., Ricketts, S., de Asis, J., White, T., Epstein, J., McBride, P. A., Eidelberg, D., Kocsis, J. H., & Silbersweig, D. A. (2000). Increased anterior cingulate and caudate activity in bipolar mania. *Biological Psychiatry*, *48*(11), 1045–1052. https://doi.org/10.1016/S0006-3223(00)00962-8

Bock, N. A., Hashim, E., Janik, R., Konyer, N. B., Weiss, M., Stanisz, G. J., Turner, R., & Geyer, S. (2013). Optimizing T1-weighted imaging of cortical myelin content at 3.0T. *NeuroImage*, *65*, 1–12. https://doi.org/10.1016/j.neuroimage.2012.09.051

Bock, N. A., Kocharyan, A., Liu, J. V., & Silva, A. C. (2009). Visualizing the entire cortical myelination pattern in marmosets with magnetic resonance imaging. *Journal of Neuroscience Methods*, *185*(1), 15–22. https://doi.org/10.1016/j.jneumeth.2009.08.022

Bojorquez, J. Z., Bricq, S., Acquitter, C., Brunotte, F., Walker, P. M., & Lalande, A. (2017). What are normal relaxation times of tissues at 3 T? *Magnetic Resonance Imaging*, *35*, 69–80. https://doi.org/10.1016/j.mri.2016.08.021

Bora, E. (2018). Neurocognitive features in clinical subgroups of bipolar disorder: A meta-analysis. *Journal of Affective Disorders*, *229*, 125–134. https://doi.org/10.1016/j.jad.2017.12.057

Boudreau, M., Tardif, C. L., Stikov, N., Sled, J. G., Lee, W., & Pike, G. B. (2017). B1 mapping for bias-correction in quantitative T1 imaging of the brain at 3T using standard pulse sequences. *Journal of Magnetic Resonance Imaging*, *46*(6), 1673–1682. https://doi.org/10.1002/jmri.25692

Bousman, C. A., Potiriadis, M., Everall, I. P., & Gunn, J. M. (2014). Effects of neuregulin-1 genetic variation and depression symptom severity on longitudinal patterns of psychotic symptoms in primary care attendees. *American Journal of Medical Genetics Part B: Neuropsychiatric Genetics*, *165*(1), 62–67.

Bradl, M., & Lassmann, H. (2010). Oligodendrocytes: Biology and pathology. *Acta Neuropathologica*, *119*(1), 37–53. https://doi.org/10.1007/s00401-009-0601-5

Cannon, D. M., Walshe, M., Dempster, E., Collier, D. A., Marshall, N., Bramon, E., Murray, R. M., & McDonald, C. (2012). The association of white matter volume in psychotic disorders with genotypic variation in NRG1, MOG and CNP: A voxel-based analysis in affected individuals and their unaffected relatives. *Translational Psychiatry*, *2*(10), e167–e167.

Cao, L., Deng, W., Guan, L., Yang, Z., Lin, Y., Ma, X., Li, X., Liu, Y., Ye, B., & Lao, G. (2014). Association of the 3′ region of the neuregulin 1 gene with bipolar I disorder in the Chinese Han population. *Journal of Affective Disorders*, *162*, 81–88.

Carriel, V., Campos, A., Alaminos, M., Raimondo, S., & Geuna, S. (2017). Staining Methods for Normal and Regenerative Myelin in the Nervous System. In C. Pellicciari & M. Biggiogera (Eds.), *Histochemistry of Single Molecules: Methods* *and Protocols* (pp. 207–218). Springer. https://doi.org/10.1007/978-1-4939-6788-9_15

Cauda, F., D'Agata, F., Sacco, K., Duca, S., Geminiani, G., & Vercelli, A. (2011). Functional connectivity of the insula in the resting brain. *NeuroImage*, *55*(1), 8–23. https://doi.org/10.1016/j.neuroimage.2010.11.049

Chen, Q., Chen, X., He, X., Wang, L., Wang, K., & Qiu, B. (2016). Aberrant structural and functional connectivity in the salience network and central executive network circuit in schizophrenia. *Neuroscience Letters*, *627*, 178–184. https://doi.org/10.1016/j.neulet.2016.05.035

Chong, V. Z., Thompson, M., Beltaifa, S., Webster, M. J., Law, A. J., & Weickert, C. S. (2008). Elevated neuregulin-1 and ErbB4 protein in the prefrontal cortex of schizophrenic patients. *Schizophrenia Research*, *100*(1), 270–280. https://doi.org/10.1016/j.schres.2007.12.474

Chou, C.-F., & Ozaki, M. (2010). In silico analysis of neuregulin 1 evolution in vertebrates. *Bioscience Reports*, *30*(4), 267–275.

Correa-Ghisays, P., Balanzá-Martínez, V., Selva-Vera, G., Vila-Francés, J., Soria-Olivas, E., Vivas-Lalinde, J., San Martín, C., Borrás, A., Ayesa-Arriola, R., Sanchez-Moreno, J., Sánchez-Ort, J., Crespo-Facorro, B., Vieta, E., & Tabarés-Seisdedos, R. (2017). Manual motor speed dysfunction as a neurocognitive endophenotype in euthymic bipolar disorder patients and their healthy relatives. Evidence from a 5-year follow-up study. *Journal of Affective Disorders*, *215*, 156–162. https://doi.org/10.1016/j.jad.2017.03.041

Deichmann, R., Good, C. D., Josephs, O., Ashburner, J., & Turner, R. (2000). Optimization of 3-D MP-RAGE Sequences for Structural Brain Imaging. *NeuroImage*, *12*(1), 112–127. https://doi.org/10.1006/nimg.2000.0601

Díez, Á., Cieza-Borrella, C., Suazo, V., González-Sarmiento, R., Papiol, S., & Molina, V. (2014). Cognitive outcome and gamma noise power unrelated to neuregulin 1 and 3 variation in schizophrenia. *Annals of General Psychiatry*, *13*(1), 1–8.

Duan, J., Wei, Y., Womer, F. Y., Zhang, X., Chang, M., Zhu, Y., Liu, Z., Li, C., Yin, Z., & Zhang, R. (2021). Neurobiological substrates of major psychiatry disorders: Transdiagnostic associations between white matter abnormalities, neuregulin 1 and clinical manifestation. *Journal of Psychiatry and Neuroscience*, *46*(5), E506–E515.

Dunayevich, E., & Keck, P. E. (2000). Prevalence and description of psychotic features in bipolar mania. *Current Psychiatry Reports*, *2*(4), 286–290. https://doi.org/10.1007/s11920-000-0069-4

Falls, D. L. (2003). Neuregulins: Functions, forms, and signaling strategies. *The EGF Receptor Family*, 15–31.

Favre, P., Pauling, M., Stout, J., Hozer, F., Sarrazin, S., Abé, C., Alda, M., Alloza, C., Alonso-Lana, S., Andreassen, O. A., Baune, B. T., Benedetti, F., Busatto, G. F., Canales-Rodríguez, E. J., Caseras, X., Chaim-Avancini, T. M., Ching, C. R. K., Dannlowski, U., Deppe, M., … Houenou, J. (2019). Widespread white matter microstructural abnormalities in bipolar disorder: Evidence from mega- and meta-analyses across 3033 individuals. *Neuropsychopharmacology*, *44*(13), Article 13.

https://doi.org/10.1038/s41386-019-0485-6

Filbin, M. T. (2003). Myelin-associated inhibitors of axonal regeneration in the adult mammalian CNS. *Nature Reviews Neuroscience*, *4*(9), Article 9. https://doi.org/10.1038/nrn1195

First, M. B. (2002). Structured clinical interview for DSM-IV-TR axis I disorders, research version, patient edition (SCID-I/P). *(No Title)*.

Fischl, B., Salat, D. H., Busa, E., Albert, M., Dieterich, M., Haselgrove, C., Van Der Kouwe, A., Killiany, R., Kennedy, D., & Klaveness, S. (2002). Whole brain segmentation: Automated labeling of neuroanatomical structures in the human brain. *Neuron*, *33*(3), 341–355.

Fonov, V. S., Evans, A. C., McKinstry, R. C., Almli, C. R., & Collins, D. L. (2009). Unbiased nonlinear average age-appropriate brain templates from birth to adulthood. *NeuroImage*, *Supplement 1*(47), S102. https://doi.org/10.1016/S1053-8119(09)70884-5

Frías, Á., Baltasar, I., & Birmaher, B. (2016). Comorbidity between bipolar disorder and borderline personality disorder: Prevalence, explanatory theories, and clinical impact. *Journal of Affective Disorders*, *202*, 210–219. https://doi.org/10.1016/j.jad.2016.05.048

Fukui, N., Muratake, T., Kaneko, N., Amagane, H., & Someya, T. (2006). Supportive evidence for neuregulin 1 as a susceptibility gene for schizophrenia in a Japanese population. *Neuroscience Letters*, *396*(2), 117–120.

Georgieva, L., Dimitrova, A., Ivanov, D., Nikolov, I., Williams, N. M., Grozeva, D., Zaharieva, I., Toncheva, D., Owen, M. J., & Kirov, G. (2008). Support for neuregulin 1 as a susceptibility gene for bipolar disorder and schizophrenia. *Biological Psychiatry*, *64*(5), 419–427.

Glasser, M. F., Coalson, T. S., Robinson, E. C., Hacker, C. D., Harwell, J., Yacoub, E., Ugurbil, K., Andersson, J., Beckmann, C. F., Jenkinson, M., Smith, S. M., & Van Essen, D. C. (2016). A multi-modal parcellation of human cerebral cortex. *Nature*, *536*(7615), Article 7615. https://doi.org/10.1038/nature18933

Glasser, M. F., Goyal, M. S., Preuss, T. M., Raichle, M. E., & Van Essen, D. C. (2014). Trends and properties of human cerebral cortex: Correlations with cortical myelin content. *NeuroImage*, *93*, 165–175. https://doi.org/10.1016/j.neuroimage.2013.03.060

Glasser, M. F., Sotiropoulos, S. N., Wilson, J. A., Coalson, T. S., Fischl, B., Andersson, J. L., Xu, J., Jbabdi, S., Webster, M., Polimeni, J. R., Van Essen, D. C., & Jenkinson, M. (2013). The minimal preprocessing pipelines for the Human Connectome Project. *NeuroImage*, *80*, 105–124. https://doi.org/10.1016/j.neuroimage.2013.04.127

Glasser, M. F., & Van Essen, D. C. (2011). Mapping human cortical areas in vivo based on myelin content as revealed by T1-and T2-weighted MRI. *Journal of Neuroscience*, *31*(32), 11597–11616.

Goes, F. S., Willour, V. L., Zandi, P. P., Belmonte, P. L., MacKinnon, D. F., Mondimore, F. M., Schweizer, B., Bipolar Disorder Phenome Group, N. G. I. B. D. C., Gershon, E. S., & McMahon, F. J. (2009). Family-based association study of

Neuregulin 1 with psychotic bipolar disorder. *American Journal of Medical Genetics Part B: Neuropsychiatric Genetics*, *150*(5), 693–702.

Gogtay, N., Giedd, J. N., Lusk, L., Hayashi, K. M., Greenstein, D., Vaituzis, A. C., Nugent, T. F., Herman, D. H., Clasen, L. S., Toga, A. W., Rapoport, J. L., & Thompson, P. M. (2004). Dynamic mapping of human cortical development during childhood through early adulthood. *Proceedings of the National Academy of Sciences*, *101*(21), 8174–8179. https://doi.org/10.1073/pnas.0402680101

Gong, J., Chen, G., Jia, Y., Zhong, S., Zhao, L., Luo, X., Qiu, S., Lai, S., Qi, Z., & Huang, L. I. (2019). Disrupted functional connectivity within the default mode network and salience network in unmedicated bipolar II disorder. *Progress in Neuro-Psychopharmacology and Biological Psychiatry*, *88*, 11–18.

Gordovez, F. J. A., & McMahon, F. J. (2020). The genetics of bipolar disorder. *Molecular Psychiatry*, *25*(3), Article 3. https://doi.org/10.1038/s41380-019-0634-7

Goulden, N., Khusnulina, A., Davis, N. J., Bracewell, R. M., Bokde, A. L., McNulty, J. P., & Mullins, P. G. (2014). The salience network is responsible for switching between the default mode network and the central executive network: Replication from DCM. *NeuroImage*, *99*, 180–190. https://doi.org/10.1016/j.neuroimage.2014.05.052

Green, E. K., Raybould, R., Macgregor, S., Gordon-Smith, K., Heron, J., Hyde, S., Grozeva, D., Hamshere, M., Williams, N., & Owen, M. J. (2005). Operation of the schizophrenia susceptibility gene, neuregulin 1, across traditional diagnostic boundaries to increase risk for bipolar disorder. *Archives of General Psychiatry*, *62*(6), 642–648.

Grydeland, H., Walhovd, K. B., Tamnes, C. K., Westlye, L. T., & Fjell, A. M. (2013). Intracortical Myelin Links with Performance Variability across the Human Lifespan: Results from T1- and T2-Weighted MRI Myelin Mapping and Diffusion Tensor Imaging. *Journal of Neuroscience*, *33*(47), 18618–18630. https://doi.org/10.1523/JNEUROSCI.2811-13.2013

Gudbjartsson, & Patz. (1995). NMR diffusion simulation based on conditional random walk. *IEEE Transactions on Medical Imaging*, *14*(4), 636–642. https://doi.org/10.1109/42.476105

Gudbjartsson, & Patz. (1995). Simultaneous calculation of flow and diffusion sensitivity in steady-state free precession imaging. *Magnetic Resonance in Medicine*, *34*(4), 567–579. https://doi.org/10.1002/mrm.1910340413

Gutiérrez-Fernández, A., Palomino, A., González-Pinto, A., Ugarte, A., Hernanz, M., Mendíbil, B., Etxebeste, M., Pacheco, L., Gónzalez-García, G., & Matute, C. (2014). Novel association of Neuregulin 1 gene with bipolar disorder but not with schizophrenia. *Schizophrenia Research*, *159*(2–3), 552–553. https://doi.org/10.1016/j.schres.2014.09.001

Haines, T. H. (2001). Do sterols reduce proton and sodium leaks through lipid bilayers? *Progress in Lipid Research*, *40*(4), 299–324. https://doi.org/10.1016/S0163-7827(01)00009-1

Hajek, T., Carrey, N., & Alda, M. (2005). Neuroanatomical abnormalities as risk factors for bipolar disorder. *Bipolar Disorders*, *7*(5), 393–403.

https://doi.org/10.1111/j.1399-5618.2005.00238.x

Hajek, T., Cullis, J., Novak, T., Kopecek, M., Blagdon, R., Propper, L., Stopkova, P., Duffy, A., Hoschl, C., Uher, R., Paus, T., Young, L. T., & Alda, M. (2013). Brain Structural Signature of Familial Predisposition for Bipolar Disorder: Replicable Evidence For Involvement of the Right Inferior Frontal Gyrus. *Biological Psychiatry*, *73*(2), 144–152. https://doi.org/10.1016/j.biopsych.2012.06.015

Hall, J., Whalley, H. C., Job, D. E., Baig, B. J., McIntosh, A. M., Evans, K. L., Thomson, P. A., Porteous, D. J., Cunningham-Owens, D. G., & Johnstone, E. C. (2006). A neuregulin 1 variant associated with abnormal cortical function and psychotic symptoms. *Nature Neuroscience*, *9*(12), 1477–1478.

Hanford, L. C., Nazarov, A., Hall, G. B., & Sassi, R. B. (2016). Cortical thickness in bipolar disorder: A systematic review. *Bipolar Disorders*, *18*(1), 4–18. https://doi.org/10.1111/bdi.12362

Harrison, & Law. (2006). Neuregulin 1 and Schizophrenia: Genetics, Gene Expression, and Neurobiology. *Biological Psychiatry*, *60*(2), 132–140. https://doi.org/10.1016/j.biopsych.2005.11.002

Hibar, D. P., Westlye, L. T., Doan, N. T., Jahanshad, N., Cheung, J. W., Ching, C. R. K., Versace, A., Bilderbeck, A. C., Uhlmann, A., Mwangi, B., Krämer, B., Overs, B., Hartberg, C. B., Abé, C., Dima, D., Grotegerd, D., Sprooten, E., Bøen, E., Jimenez, E., … Andreassen, O. A. (2018). Cortical abnormalities in bipolar disorder: An MRI analysis of 6503 individuals from the ENIGMA Bipolar Disorder Working Group. *Molecular Psychiatry*, *23*(4), Article 4.

https://doi.org/10.1038/mp.2017.73

Ho, N. F., Li, Z., Ji, F., Wang, M., Kuswanto, C. N., Sum, M. Y., Tng, H. Y., Sitoh, Y. Y., Sim, K., & Zhou, J. (2017). Hemispheric lateralization abnormalities of the white matter microstructure in patients with schizophrenia and bipolar disorder. *Journal of Psychiatry and Neuroscience*, *42*(4), 242–251. https://doi.org/10.1503/jpn.160090

Hof, P. R., Haroutunian, V., Copland, C., Davis, K. L., & Buxbaum, J. D. (2002). Molecular and Cellular Evidence for an Oligodendrocyte Abnormality in Schizophrenia. *Neurochemical Research*, *27*(10), 1193–1200. https://doi.org/10.1023/A:1020981510759

Houenou, J., Wessa, M., Douaud, G., Leboyer, M., Chanraud, S., Perrin, M., Poupon, C., Martinot, J.-L., & Paillere-Martinot, M.-L. (2007). Increased white matter connectivity in euthymic bipolar patients: Diffusion tensor tractography between the subgenual cingulate and the amygdalo-hippocampal complex. *Molecular Psychiatry*, *12*(11), Article 11. https://doi.org/10.1038/sj.mp.4002010

Jenkinson, M., Beckmann, C. F., Behrens, T. E. J., Woolrich, M. W., & Smith, S. M. (2012). FSL. *NeuroImage*, *62*(2), 782–790. https://doi.org/10.1016/j.neuroimage.2011.09.015

Jørgensen, K. N., Nerland, S., Norbom, L. B., Doan, N. T., Nesvåg, R., Mørch-Johnsen, L., Haukvik, U. K., Melle, I., Andreassen, O. A., Westlye, L. T., & Agartz, I. (2016). Increased MRI-based cortical grey/white-matter contrast in sensory and motor regions in schizophrenia and bipolar disorder. *Psychological Medicine*, *46*(9), 1971–1985. https://doi.org/10.1017/S0033291716000593

Joslyn, C., Hawes, D. J., Hunt, C., & Mitchell, P. B. (2016). Is age of onset associated with severity, prognosis, and clinical features in bipolar disorder? A meta-analytic review. *Bipolar Disorders*, *18*(5), 389–403. https://doi.org/10.1111/bdi.12419

Karakuzu, A., Biswas, L., Cohen-Adad, J., & Stikov, N. (2022). Vendor-neutral sequences and fully transparent workflows improve inter-vendor reproducibility of quantitative MRI. *Magnetic Resonance in Medicine*, *88*(3), 1212–1228. https://doi.org/10.1002/mrm.29292

Kataria, H., Alizadeh, A., & Karimi-Abdolrezaee, S. (2019). Neuregulin-1/ErbB network: An emerging modulator of nervous system injury and repair. *Progress in Neurobiology*, *180*, 101643.

Kemper, T. L. (1994). Neuroanatomical and neuropathological changes during aging and dementia. In *Clinical neurology of aging, 2nd ed* (pp. 3–67). Oxford University Press.

Kéri, S., Kiss, I., Seres, I., & Kelemen, O. (2009). A polymorphism of the neuregulin 1 gene (SNP8NRG243177/rs6994992) affects reactivity to expressed emotion in schizophrenia. *American Journal of Medical Genetics Part B: Neuropsychiatric Genetics*, *150*(3), 418–420.

Khare, P., Raj, V., Chandra, S., & Agarwal, S. (2014). Quantitative and qualitative assessment of DNA extracted from saliva for its use in forensic identification. *Journal of Forensic Dental Sciences*, *6*(2), 81.

Kim, S., & Webster, M. J. (2010). Correlation analysis between genome-wide expression profiles and cytoarchitectural abnormalities in the prefrontal cortex of psychiatric disorders. *Molecular Psychiatry*, *15*(3), Article 3. https://doi.org/10.1038/mp.2008.99

Kukshal, P., Bhatia, T., Bhagwat, A. M., Gur, R. E., Gur, R. C., Deshpande, S. N., Nimgaonkar, V. L., & Thelma, B. K. (2013). Association study of neuregulin-1 gene polymorphisms in a North Indian schizophrenia sample. *Schizophrenia Research*, *144*(1–3), 24–30.

Kuperberg, G. R., Broome, M. R., McGuire, P. K., David, A. S., Eddy, M., Ozawa, F., Goff, D., West, W. C., Williams, S. C. R., van der Kouwe, A. J. W., Salat, D. H., Dale, A. M., & Fischl, B. (2003). Regionally Localized Thinning of the Cerebral Cortex in Schizophrenia. *Archives of General Psychiatry*, *60*(9), 878–888. https://doi.org/10.1001/archpsyc.60.9.878

Lake, E. M. R., Steffler, E. A., Rowley, C. D., Sehmbi, M., Minuzzi, L., Frey, B. N., & Bock, N. A. (2017). Altered intracortical myelin staining in the dorsolateral prefrontal cortex in severe mental illness. *European Archives of Psychiatry and Clinical Neuroscience*, *267*(5), 369–376. https://doi.org/10.1007/s00406-016-0730-5

Law, A. J., Lipska, B. K., Weickert, C. S., Hyde, T. M., Straub, R. E., Hashimoto, R., Harrison, P. J., Kleinman, J. E., & Weinberger, D. R. (2006). Neuregulin 1 transcripts are differentially expressed in schizophrenia and regulated by 5′ SNPs associated with the disease. *Proceedings of the National Academy of Sciences*, *103*(17), 6747–6752.

Law, A. J., Weickert, C. S., Hyde, T. M., Kleinman, J. E., & Harrison, P. J. (2004). Neuregulin-1 (NRG-1) mRNA and protein in the adult human brain. *Neuroscience*, *127*(1), 125–136.

Ledonne, A., & Mercuri, N. B. (2020). On the Modulatory Roles of Neuregulins/ErbB Signaling on Synaptic Plasticity. *International Journal of Molecular Sciences*, *21*(1), Article 1. https://doi.org/10.3390/ijms21010275

Levy, B., Medina, A. M., & Weiss, R. D. (2013). Cognitive and psychosocial functioning in bipolar disorder with and without psychosis during early remission from an acute mood episode: A comparative longitudinal study. *Comprehensive Psychiatry*, *54*(6), 618–626. https://doi.org/10.1016/j.comppsych.2012.12.018

Li, D., Collier, D. A., & He, L. (2006). Meta-analysis shows strong positive association of the neuregulin 1 (NRG1) gene with schizophrenia. *Human Molecular Genetics*, *15*(12), 1995–2002.

Liu, Bates, R., Yin, D.-M., Shen, C., Wang, F., Su, N., Kirov, S. A., Luo, Y., Wang, J.-Z., Xiong, W.-C., & Mei, L. (2011). Specific Regulation of NRG1 Isoform Expression by Neuronal Activity. *The Journal of Neuroscience*, *31*(23), 8491–8501. https://doi.org/10.1523/JNEUROSCI.5317-10.2011

Liu, Ford, B., Mann, M. A., & Fischbach, G. D. (2001). Neuregulins increase α7 nicotinic acetylcholine receptors and enhance excitatory synaptic transmission in GABAergic interneurons of the hippocampus. *Journal of Neuroscience*, *21*(15), 5660–5669.

Lopez-Larson, M. P., Shah, L. M., Weeks, H. R., King, J. B., Mallik, A. K., Yurgelun-

Todd, D. A., & Anderson, J. S. (2017). Abnormal functional connectivity between default and salience networks in pediatric bipolar disorder. *Biological Psychiatry: Cognitive Neuroscience and Neuroimaging*, *2*(1), 85–93.

Lubeiro, A., Gomez-Pilar, J., Martín, O., Palomino, A., Fernández, M., González-Pinto, A., Poza, J., Hornero, R., & Molina, V. (2017). Variation at NRG1 genotype related to modulation of small-world properties of the functional cortical network. *European Archives of Psychiatry and Clinical Neuroscience*, *267*, 25–32.

Luo, Li, L., Guo, M., Chen, X., Lin, Y., & Wu, D. (2020). Genetic variation in NRG 1 gene and risk of post-traumatic stress disorders in patients with hepatocellular carcinoma. *Journal of Clinical Laboratory Analysis*, *34*(5), e23187.

Luo, Qin, S., Fernández, G., Zhang, Y., Klumpers, F., & Li, H. (2014). Emotion perception and executive control interact in the salience network during emotionally charged working memory processing. *Human Brain Mapping*, *35*(11), 5606–5616. https://doi.org/10.1002/hbm.22573

Margulies, D. S., Kelly, A. M. C., Uddin, L. Q., Biswal, B. B., Castellanos, F. X., & Milham, M. P. (2007). Mapping the functional connectivity of anterior cingulate cortex. *NeuroImage*, *37*(2), 579–588. https://doi.org/10.1016/j.neuroimage.2007.05.019

Marlinge, E., Bellivier, F., & Houenou, J. (2014). White matter alterations in bipolar disorder: Potential for drug discovery and development. *Bipolar Disorders*, *16*(2), 97–112. https://doi.org/10.1111/bdi.12135

Marques, J. P., & Gruetter, R. (2013). New Developments and Applications of the

MP2RAGE Sequence—Focusing the Contrast and High Spatial Resolution R1 Mapping. *PLOS ONE*, *8*(7), e69294. https://doi.org/10.1371/journal.pone.0069294

Marques, J. P., Kober, T., Krueger, G., van der Zwaag, W., Van de Moortele, P.-F., & Gruetter, R. (2010). MP2RAGE, a self bias-field corrected sequence for improved segmentation and T1-mapping at high field. *NeuroImage*, *49*(2), 1271–1281. https://doi.org/10.1016/j.neuroimage.2009.10.002

McDonald, C., Bullmore, E. T., Sham, P. C., Chitnis, X., Wickham, H., Bramon, E., & Murray, R. M. (2004). Association of Genetic Risks for Schizophrenia and Bipolar DisorderWith Specific and Generic Brain Structural Endophenotypes. *Archives of General Psychiatry*, *61*(10), 974–984. https://doi.org/10.1001/archpsyc.61.10.974

McGee, A. W., Yang, Y., Fischer, Q. S., Daw, N. W., & Strittmatter, S. M. (2005). Experience-Driven Plasticity of Visual Cortex Limited by Myelin and Nogo Receptor. *Science*, *309*(5744), 2222–2226. https://doi.org/10.1126/science.1114362

McIntosh, A. M., Moorhead, T. W. J., Job, D., Lymer, G. K. S., Munoz Maniega, S., McKirdy, J., Sussmann, J. E. D., Baig, B. J., Bastin, M. E., & Porteous, D. (2008). The effects of a neuregulin 1 variant on white matter density and integrity. *Molecular Psychiatry*, *13*(11), 1054–1059.

McKenzie, I. A., Ohayon, D., Li, H., de Faria, J. P., Emery, B., Tohyama, K., & Richardson, W. D. (2014). Motor skill learning requires active central myelination. *Science (New York, N.Y.)*, *346*(6207), 318–322.

https://doi.org/10.1126/science.1254960

Mechelli, A., Prata, D. P., Fu, C. H., Picchioni, M., Kane, F., Kalidindi, S., McDonald, C., Demjaha, A., Kravariti, E., & Toulopoulou, T. (2008). The effects of neuregulin1 on brain function in controls and patients with schizophrenia and bipolar disorder. *Neuroimage*, *42*(2), 817–826.

Menon, V. (2011). Large-scale brain networks and psychopathology: A unifying triple network model. *Trends in Cognitive Sciences*, *15*(10), 483–506. https://doi.org/10.1016/j.tics.2011.08.003

Merikangas, K. R., Jin, R., He, J.-P., Kessler, R. C., Lee, S., Sampson, N. A., Viana, M. C., Andrade, L. H., Hu, C., Karam, E. G., Ladea, M., Medina-Mora, M. E., Ono, Y., Posada-Villa, J., Sagar, R., Wells, J. E., & Zarkov, Z. (2011). Prevalence and Correlates of Bipolar Spectrum Disorder in the World Mental Health Survey Initiative. *Archives of General Psychiatry*, *68*(3), 241–251. https://doi.org/10.1001/archgenpsychiatry.2011.12

Micheva, K. D., Wolman, D., Mensh, B. D., Pax, E., Buchanan, J., Smith, S. J., & Bock, D. D. (2016). A large fraction of neocortical myelin ensheathes axons of local inhibitory neurons. *ELife*, *5*, e15784. https://doi.org/10.7554/eLife.15784

Montgomery, S. A., & Åsberg, M. (1979). A new depression scale designed to be sensitive to change. *The British Journal of Psychiatry*, *134*(4), 382–389.

Moon, E., Rollins, B., Mesén, A., Sequeira, A., Myers, R. M., Akil, H., Watson, S. J., Barchas, J., Jones, E. G., Schatzberg, A., Bunney, W. E., DeLisi, L. E., Byerley, W., & Vawter, M. P. (2011). Lack of association to a NRG1 missense polymorphism in schizophrenia or bipolar disorder in a Costa Rican population. *Schizophrenia Research*, *131*(1), 52–57. https://doi.org/10.1016/j.schres.2011.06.024

Morell, P., & Quarles, R. H. (1999). The Myelin Sheath. In *Basic Neurochemistry: Molecular, Cellular and Medical Aspects. 6th edition*. Lippincott-Raven. https://www.ncbi.nlm.nih.gov/books/NBK27954/

Morris, V., Bock, N., Minuzzi, L., MacKillop, J., & Amlung, M. (2022). Intracortical myelin in individuals with alcohol use disorder: An initial proof-of-concept study. *Brain and Behavior*, *12*(10), e2762. https://doi.org/10.1002/brb3.2762

Mostaid, M. S., Lloyd, D., Liberg, B., Sundram, S., Pereira, A., Pantelis, C., Karl, T., Weickert, C. S., Everall, I. P., & Bousman, C. A. (2016). Neuregulin-1 and schizophrenia in the genome-wide association study era. *Neuroscience & Biobehavioral Reviews*, *68*, 387–409.

Negash, A., Kebede, D., Alem, A., Melaku, Z., Deyessa, N., Shibire, T., Fekadu, A., Fekadu, D., Jacobsson, L., & Kullgren, G. (2004). Neurological soft signs in bipolar I disorder patients. *Journal of Affective Disorders*, *80*(2), 221–230. https://doi.org/10.1016/S0165-0327(03)00116-2

Nerland, S., Jørgensen, K. N., Nordhøy, W., Maximov, I. I., Bugge, R. A. B., Westlye, L. T., Andreassen, O. A., Geier, O. M., & Agartz, I. (2021). Multisite reproducibility and test-retest reliability of the T1w/T2w-ratio: A comparison of processing methods. *NeuroImage*, *245*, 118709. https://doi.org/10.1016/j.neuroimage.2021.118709

Nery, F. G., Chen, H.-H., Hatch, J. P., Nicoletti, M. A., Brambilla, P., Sassi, R. B., Mallinger, A. G., Keshavan, M. S., & Soares, J. C. (2009). Orbitofrontal cortex gray matter volumes in bipolar disorder patients: A region-of-interest MRI study. *Bipolar Disorders*, *11*(2), 145–153. https://doi.org/10.1111/j.1399-5618.2009.00662.x

Nierenberg, A. A., Miyahara, S., Spencer, T., Wisniewski, S. R., Otto, M. W., Simon, N., Pollack, M. H., Ostacher, M. J., Yan, L., Siegel, R., & Sachs, G. S. (2005). Clinical and Diagnostic Implications of Lifetime Attention-Deficit/Hyperactivity Disorder Comorbidity in Adults with Bipolar Disorder: Data from the First 1000 STEP-BD Participants. *Biological Psychiatry*, *57*(11), 1467–1473. https://doi.org/10.1016/j.biopsych.2005.01.036

Nieuwenhuys, R. (2013). The Myeloarchitectonic Studies on the Human Cerebral Cortex of the Vogt-Vogt School, and Their Significance for the Interpretation of Functional Neuroimaging Data. In S. Geyer & R. Turner (Eds.), *Microstructural Parcellation of the Human Cerebral Cortex: From Brodmann's Post-Mortem Map to in Vivo Mapping with High-Field Magnetic Resonance Imaging* (pp. 55–125). Springer. https://doi.org/10.1007/978-3-642-37824-9_3

O'Brien, J. S. (1965). Stability of the Myelin Membrane. *Science*, *147*(3662), 1099–1107.

Ohvo-Rekilä, H., Ramstedt, B., Leppimäki, P., & Peter Slotte, J. (2002). Cholesterol interactions with phospholipids in membranes. *Progress in Lipid Research*, *41*(1), 66–97. https://doi.org/10.1016/S0163-7827(01)00020-0

Öngür, D., Drevets, W. C., & Price, J. L. (1998). Glial reduction in the subgenual prefrontal cortex in mood disorders. *Proceedings of the National Academy of Sciences*, *95*(22), 13290–13295. https://doi.org/10.1073/pnas.95.22.13290

Ozaki, M., Sasner, M., Yano, R., Lu, H. S., & Buonanno, A. (1997). Neuregulin-β induces expression of an NMDA-receptor subunit. *Nature*, *390*(6661), Article 6661. https://doi.org/10.1038/37795

Pajevic, S., Basser, P. J., & Fields, R. D. (2014). Role of myelin plasticity in oscillations and synchrony of neuronal activity. *Neuroscience*, *276*, 135–147. https://doi.org/10.1016/j.neuroscience.2013.11.007

Pan, S., Mayoral, S. R., Choi, H. S., Chan, J. R., & Kheirbek, M. A. (2020). Preservation of a remote fear memory requires new myelin formation. *Nature Neuroscience*, *23*(4), Article 4. https://doi.org/10.1038/s41593-019-0582-1

Pavlova, B., Perlis, R. H., Alda, M., & Uher, R. (2015). Lifetime prevalence of anxiety disorders in people with bipolar disorder: A systematic review and meta-analysis. *The Lancet Psychiatry*, *2*(8), 710–717. https://doi.org/10.1016/S2215-0366(15)00112-1

Poletti, S., Bollettini, I., Mazza, E., Locatelli, C., Radaelli, D., Vai, B., Smeraldi, E., Colombo, C., & Benedetti, F. (2015). Cognitive performances associate with measures of white matter integrity in bipolar disorder. *Journal of Affective Disorders*, *174*, 342–352. https://doi.org/10.1016/j.jad.2014.12.030

Prata, D. P., Breen, G., Osborne, S., Munro, J., Clair, D. S., & Collier, D. A. (2009). An association study of the neuregulin 1 gene, bipolar affective disorder and psychosis. *Psychiatric Genetics*, *19*(3), 113.

https://doi.org/10.1097/YPG.0b013e32832a4f69

Quarles, R. H., Macklin, W. B., & Morell, P. (2006). Myelin formation, structure and biochemistry. *Basic Neurochemistry: Molecular, Cellular and Medical Aspects*, *7*, 51–71.

Rieff, H. I., Raetzman, L. T., Sapp, D. W., Yeh, H. H., Siegel, R. E., & Corfas, G. (1999). Neuregulin Induces GABA $_{A}$ Receptor Subunit Expression and Neurite Outgrowth in Cerebellar Granule Cells. *The Journal of Neuroscience*, *19*(24), 10757–10766. https://doi.org/10.1523/JNEUROSCI.19-24-10757.1999

Rolstad, S., Pålsson, E., Ekman, C. J., Eriksson, E., Sellgren, C., & Landén, M. (2015). Polymorphisms of dopamine pathway genes NRG1 and LMX1A are associated with cognitive performance in bipolar disorder. *Bipolar Disorders*, *17*(8), 859–868. https://doi.org/10.1111/bdi.12347

Rosa, A. R., Sánchez-Moreno, J., Martínez-Aran, A., Salamero, M., Torrent, C., Reinares, M., Comes, M., Colom, F., Van Riel, W., & Ayuso-Mateos, J. L. (2007). Validity and reliability of the Functioning Assessment Short Test (FAST) in bipolar disorder. *Clinical Practice and Epidemiology in Mental Health*, *3*(1), 1–8.

Rowley, C. D., Bazin, P.-L., Tardif, C. L., Sehmbi, M., Hashim, E., Zaharieva, N., Minuzzi, L., Frey, B. N., & Bock, N. A. (2015). Assessing intracortical myelin in the living human brain using myelinated cortical thickness. *Frontiers in Neuroscience*, *9*. https://www.frontiersin.org/articles/10.3389/fnins.2015.00396

Rowley, C. D., Sehmbi, M., Bazin, P.-L., Tardif, C. L., Minuzzi, L., Frey, B. N., & Bock, N. A. (2017). Age-related mapping of intracortical myelin from late adolescence to middle adulthood using T1-weighted MRI. *Human Brain Mapping*, *38*(7), 3691–3703.

Roy, K., Murtie, J. C., El-Khodor, B. F., Edgar, N., Sardi, S. P., Hooks, B. M., Benoit-Marand, M., Chen, C., Moore, H., O'Donnell, P., Brunner, D., & Corfas, G. (2007). Loss of erbB signaling in oligodendrocytes alters myelin and dopaminergic function, a potential mechanism for neuropsychiatric disorders. *Proceedings of the National Academy of Sciences*, *104*(19), 8131–8136. https://doi.org/10.1073/pnas.0702157104

Sacchet, M. D., & Gotlib, I. H. (2017). Myelination of the brain in major depressive disorder: An in vivo quantitative magnetic resonance imaging study. *Scientific Reports*, *7*(1), 1–14.

Sacolick, L. I., Wiesinger, F., Hancu, I., & Vogel, M. W. (2010). B1 mapping by Bloch-Siegert shift. *Magnetic Resonance in Medicine*, *63*(5), 1315–1322. https://doi.org/10.1002/mrm.22357

Salat, D. H., Lee, S. Y., van der Kouwe, A. J., Greve, D. N., Fischl, B., & Rosas, H. D. (2009). Age-associated alterations in cortical gray and white matter signal intensity and gray to white matter contrast. *NeuroImage*, *48*(1), 21–28. https://doi.org/10.1016/j.neuroimage.2009.06.074

Samalin, L., de Chazeron, I., Vieta, E., Bellivier, F., & Llorca, P.-M. (2016). Residual symptoms and specific functional impairments in euthymic patients with bipolar disorder. *Bipolar Disorders*, *18*(2), 164–173. https://doi.org/10.1111/bdi.12376

Sanchez-Moreno, J., Martinez-Aran, A., Tabarés-Seisdedos, R., Torrent, C., Vieta, E., &

Ayuso-Mateos, J. L. (2009). Functioning and Disability in Bipolar Disorder: An Extensive Review. *Psychotherapy and Psychosomatics*, *78*(5), 285–297.

Sanides, F. (1969). Comparative Architectonics of the Neocortex of Mammals and Their Evolutionary Interpretation*. *Annals of the New York Academy of Sciences*, *167*(1), 404–423. https://doi.org/10.1111/j.1749-6632.1969.tb20459.x

Savitz, J. B., Price, J. L., & Drevets, W. C. (2014). Neuropathological and neuromorphometric abnormalities in bipolar disorder: View from the medial prefrontal cortical network. *Neuroscience & Biobehavioral Reviews*, *42*, 132–147. https://doi.org/10.1016/j.neubiorev.2014.02.008

Schaum, M., Pinzuti, E., Sebastian, A., Lieb, K., Fries, P., Mobascher, A., Jung, P., Wibral, M., & Tüscher, O. (2021). Right inferior frontal gyrus implements motor inhibitory control via beta-band oscillations in humans. *ELife*, *10*, e61679. https://doi.org/10.7554/eLife.61679

Schmierer, K., Scaravilli, F., Altmann, D. R., Barker, G. J., & Miller, D. H. (2004). Magnetization transfer ratio and myelin in postmortem multiple sclerosis brain. *Annals of Neurology*, *56*(3), 407–415. https://doi.org/10.1002/ana.20202

Schmitt, J. E., Raznahan, A., Liu, S., & Neale, M. C. (2020). The genetics of cortical myelination in young adults and its relationships to cerebral surface area, cortical thickness, and intelligence: A magnetic resonance imaging study of twins and families. *NeuroImage*, *206*, 116319. https://doi.org/10.1016/j.neuroimage.2019.116319

Seeley, W. W., Menon, V., Schatzberg, A. F., Keller, J., Glover, G. H., Kenna, H., Reiss,

A. L., & Greicius, M. D. (2007). Dissociable Intrinsic Connectivity Networks for Salience Processing and Executive Control. *Journal of Neuroscience*, *27*(9), 2349–2356. https://doi.org/10.1523/JNEUROSCI.5587-06.2007

Sehmbi, M., Rowley, C. D., Minuzzi, L., Kapczinski, F., Kwiecien, J. M., Bock, N. A., & Frey, B. N. (2019). Age-related deficits in intracortical myelination in young adults with bipolar disorder type I. *Journal of Psychiatry and Neuroscience*, *44*(2), 79–88. https://doi.org/10.1503/jpn.170220

Sehmbi, M., Rowley, C. D., Minuzzi, L., Kapczinski, F., Steiner, M., Sassi, R. B., Bock, N. A., & Frey, B. N. (2018). Association of intracortical myelin and cognitive function in bipolar I disorder. *Acta Psychiatrica Scandinavica*, *138*(1), 62–72. https://doi.org/10.1111/acps.12875

Sehmbi, M., Suh, J. S., Rowley, C. D., Minuzzi, L., Kapczinski, F., Bock, N. A., & Frey, B. N. (2022). Network properties of intracortical myelin associated with psychosocial functioning in bipolar I disorder. *Bipolar Disorders*, *24*(5), 539–548. https://doi.org/10.1111/bdi.13181

Selvaraj, S., Arnone, D., Job, D., Stanfield, A., Farrow, T. F., Nugent, A. C., Scherk, H., Gruber, O., Chen, X., Sachdev, P. S., Dickstein, D. P., Malhi, G. S., Ha, T. H., Ha, K., Phillips, M. L., & McIntosh, A. M. (2012). Grey matter differences in bipolar disorder: A meta-analysis of voxel-based morphometry studies. *Bipolar Disorders*, *14*(2), 135–145. https://doi.org/10.1111/j.1399-5618.2012.01000.x

Sereno, M. I., Lutti, A., Weiskopf, N., & Dick, F. (2013). Mapping the Human Cortical Surface by Combining Quantitative T1 with Retinotopy†. *Cerebral Cortex*, *23*(9), 2261–2268. https://doi.org/10.1093/cercor/bhs213

Shamir, A., & Buonanno, A. (2010). Molecular and cellular characterization of Neuregulin-1 type IV isoforms. *Journal of neurochemistry*, *113*(5), 1163–1176. https://doi.org/10.1111/j.1471-4159.2010.06677.x

Shams, Z., Norris, D. G., & Marques, J. P. (2019). A comparison of in vivo MRI based cortical myelin mapping using T1w/T2w and R1 mapping at 3T. *PLOS ONE*, *14*(7), e0218089. https://doi.org/10.1371/journal.pone.0218089

Shine, H. D., Readhead, C., Popko, B., Hood, L., & Sidman, R. L. (1992). Morphometric Analysis of Normal, Mutant, and Transgenic CNS: Correlation of Myelin Basic Protein Expression to Myelinogenesis. *Journal of Neurochemistry*, *58*(1), 342–349. https://doi.org/10.1111/j.1471-4159.1992.tb09316.x

Simon, N. M., Otto, M. W., Wisniewski, S. R., Fossey, M., Sagduyu, K., Frank, E., Sachs, G. S., Nierenberg, A. A., Thase, M. E., & Pollack, M. H. (2004). Anxiety Disorder Comorbidity in Bipolar Disorder Patients: Data From the First 500 Participants in the Systematic Treatment Enhancement Program for Bipolar Disorder (STEP-BD). *American Journal of Psychiatry*, *161*(12), 2222–2229. https://doi.org/10.1176/appi.ajp.161.12.2222

Smoller, J. W., & Finn, C. T. (2003). Family, twin, and adoption studies of bipolar disorder. *American Journal of Medical Genetics Part C: Seminars in Medical Genetics*, *123C*(1), 48–58. https://doi.org/10.1002/ajmg.c.20013

Sprooten, E., Lymer, G. K. S., Maniega, S. M., McKirdy, J., Clayden, J. D., Bastin, M. E., Porteous, D., Johnstone, E. C., Lawrie, S. M., Hall, J., & McIntosh, A. M.

(2009). The relationship of anterior thalamic radiation integrity to psychosis risk associated neuregulin-1 variants. *Molecular Psychiatry*, *14*(3), Article 3. https://doi.org/10.1038/mp.2008.136

Sridharan, D., Levitin, D. J., & Menon, V. (2008). A critical role for the right fronto-insular cortex in switching between central-executive and default-mode networks. *Proceedings of the National Academy of Sciences*, *105*(34), 12569–12574. https://doi.org/10.1073/pnas.0800005105

Stahl, E. A., Breen, G., Forstner, A. J., McQuillin, A., Ripke, S., Trubetskoy, V., Mattheisen, M., Wang, Y., Coleman, J. R. I., Gaspar, H. A., de Leeuw, C. A., Steinberg, S., Pavlides, J. M. W., Trzaskowski, M., Byrne, E. M., Pers, T. H., Holmans, P. A., Richards, A. L., Abbott, L., … Sklar, P. (2019). Genome-wide association study identifies 30 loci associated with bipolar disorder. *Nature Genetics*, *51*(5), Article 5. https://doi.org/10.1038/s41588-019-0397-8

Stefanis, N. C., Trikalinos, T. A., Avramopoulos, D., Smyrnis, N., Evdokimidis, I., Ntzani, E. E., Ioannidis, J. P., & Stefanis, C. N. (2007). Impact of Schizophrenia Candidate Genes on Schizotypy and Cognitive Endophenotypes at the Population Level. *Biological Psychiatry*, *62*(7), 784–792. https://doi.org/10.1016/j.biopsych.2006.11.015

Stefansson, H., Petursson, H., Sigurdsson, E., Steinthorsdottir, V., Bjornsdottir, S., Sigmundsson, T., Ghosh, S., Brynjolfsson, J., Gunnarsdottir, S., Ivarsson, O., Chou, T. T., Hjaltason, O., Birgisdottir, B., Jonsson, H., Gudnadottir, V. G., Gudmundsdottir, E., Bjornsson, A., Ingvarsson, B., Ingason, A., … Stefansson, K.

(2002). Neuregulin 1 and Susceptibility to Schizophrenia. *The American Journal of Human Genetics*, *71*(4), 877–892. https://doi.org/10.1086/342734

Stefansson, H., Sarginson, J., Kong, A., Yates, P., Steinthorsdottir, V., Gudfinnsson, E., Gunnarsdottir, S., Walker, N., Petursson, H., Crombie, C., Ingason, A., Gulcher, J. R., Stefansson, K., & Clair, D. S. (2003). Association of Neuregulin 1 with Schizophrenia Confirmed in a Scottish Population. *The American Journal of Human Genetics*, *72*(1), 83–87. https://doi.org/10.1086/345442

Suarez-Pinilla, P., Roiz-Santiañez, R., Mata, I., Ortiz-García de la Foz, V., Brambilla, P., Fañanás, L., Román, N., & Crespo-Facorro, B. (2015). Progressive Structural Brain Changes and NRG1 Gene Variants in First-Episode Nonaffective Psychosis. *Neuropsychobiology*, *71*, 103–111. https://doi.org/10.1159/000370075

Sussmann, J. E., Lymer, G. K. S., McKirdy, J., Moorhead, T. W. J., Maniega, S. M., Job, D., Hall, J., Bastin, M. E., Johnstone, E. C., Lawrie, S. M., & McIntosh, A. M. (2009). White matter abnormalities in bipolar disorder and schizophrenia detected using diffusion tensor magnetic resonance imaging. *Bipolar Disorders*, *11*(1), 11–18. https://doi.org/10.1111/j.1399-5618.2008.00646.x

Swann, N. C., Cai, W., Conner, C. R., Pieters, T. A., Claffey, M. P., George, J. S., Aron, A. R., & Tandon, N. (2012). Roles for the pre-supplementary motor area and the right inferior frontal gyrus in stopping action: Electrophysiological responses and functional and structural connectivity. *NeuroImage*, *59*(3), 2860–2870. https://doi.org/10.1016/j.neuroimage.2011.09.049

Swinehart, D. F. (1962). The beer-lambert law. *Journal of Chemical Education*, *39*(7), 333.

Tan, W., Wang, Y., Gold, B., Chen, J., Dean, M., Harrison, P. J., Weinberger, D. R., & Law, A. J. (2007). Molecular Cloning of a Brain-specific, Developmentally Regulated Neuregulin 1 (NRG1) Isoform and Identification of a Functional Promoter Variant Associated with Schizophrenia * ♦. *Journal of Biological Chemistry*, *282*(33), 24343–24351. https://doi.org/10.1074/jbc.M702953200

Timmler, S., & Simons, M. (2019). Grey matter myelination. *Glia*, *67*(11), 2063–2070. https://doi.org/10.1002/glia.23614

Tishler, T. A., Bartzokis, G., Lu, P. H., Raven, E. P., Khanoyan, M., Kirkpatrick, C. J., Pyle, M. H., Villablanca, J. P., Altshuler, L. L., Mintz, J., Ventura, J., Casaus, L. R., Subotnik, K. L., Nuechterlein, K. H., & Ellingson, B. M. (2018). Abnormal Trajectory of Intracortical Myelination in Schizophrenia Implicates White Matter in Disease Pathophysiology and the Therapeutic Mechanism of Action of Antipsychotics. *Biological Psychiatry: Cognitive Neuroscience and Neuroimaging*, *3*(5), 454–462. https://doi.org/10.1016/j.bpsc.2017.03.007

Tkachev, D., Mimmack, M. L., Ryan, M. M., Wayland, M., Freeman, T., Jones, P. B., Starkey, M., Webster, M. J., Yolken, R. H., & Bahn, S. (2003). Oligodendrocyte dysfunction in schizophrenia and bipolar disorder. *The Lancet*, *362*(9386), 798–805. https://doi.org/10.1016/S0140-6736(03)14289-4

Townsend, J. D., Bookheimer, S. Y., Foland-Ross, L. C., Moody, T. D., Eisenberger, N. I., Fischer, J. S., Cohen, M. S., Sugar, C. A., & Altshuler, L. L. (2012). Deficits in inferior frontal cortex activation in euthymic bipolar disorder patients during a response inhibition task. *Bipolar Disorders*, *14*(4), 442–450. https://doi.org/10.1111/j.1399-5618.2012.01020.x

Vargas, C., López-Jaramillo, C., & Vieta, E. (2013). A systematic literature review of resting state network—Functional MRI in bipolar disorder. *Journal of Affective Disorders*, *150*(3), 727–735. https://doi.org/10.1016/j.jad.2013.05.083

Vidal-Piñeiro, D., Walhovd, K. B., Storsve, A. B., Grydeland, H., Rohani, D. A., & Fjell, A. M. (2016). Accelerated longitudinal gray/white matter contrast decline in aging in lightly myelinated cortical regions. *Human Brain Mapping*, *37*(10), 3669–3684. https://doi.org/10.1002/hbm.23267

Vigo, D., Thornicroft, G., & Atun, R. (2016). Estimating the true global burden of mental illness. *The Lancet Psychiatry*, *3*(2), 171–178. https://doi.org/10.1016/S2215-0366(15)00505-2

Vostrikov, Uranova, N. A., & Orlovskaya, D. D. (2007). Deficit of perineuronal oligodendrocytes in the prefrontal cortex in schizophrenia and mood disorders. *Schizophrenia Research*, *94*(1), 273–280. https://doi.org/10.1016/j.schres.2007.04.014

Wang, F., Jiang, T., Sun, Z., Teng, S., Luo, X., Zhu, Z., Zang, Y., Zhang, H., Yue, W., Qu, M., Lu, T., Hong, N., Huang, H., Blumberg, H. P., & Zhang, D. (2009). Neuregulin 1 genetic variation and anterior cingulum integrity in patients with schizophrenia and healthy controls. *Journal of Psychiatry and Neuroscience*, *34*(3), 181–186.

Wei, W., Zhang, Y., Li, Y., Meng, Y., Li, M., Wang, Q., Deng, W., Ma, X., Palaniyappan, L., Zhang, N., & Li, T. (2020). Depth-dependent abnormal cortical myelination in first-episode treatment-naïve schizophrenia. *Human Brain Mapping*, *41*(10), 2782–2793. https://doi.org/10.1002/hbm.24977

Weiskopf, N., Suckling, J., Williams, G., Correia, M., Inkster, B., Tait, R., Ooi, C., Bullmore, E., & Lutti, A. (2013). Quantitative multi-parameter mapping of R1, PD*, MT, and R2* at 3T: A multi-center validation. *Frontiers in Neuroscience*, *7*. https://www.frontiersin.org/articles/10.3389/fnins.2013.00095

Wen, Z., Chen, J., Khan, R. A. W., Song, Z., Wang, M., Li, Z., Shen, J., Li, W., & Shi, Y. (2016). Genetic association between NRG1 and schizophrenia, major depressive disorder, bipolar disorder in Han Chinese population. *American Journal of Medical Genetics Part B: Neuropsychiatric Genetics*, *171*(3), 468–478. https://doi.org/10.1002/ajmg.b.32428

Wessa, M., Houenou, J., Paillère-Martinot, M.-L., Berthoz, S., Artiges, E., Leboyer, M., & Martinot, J.-L. (2007). Fronto-Striatal Overactivation in Euthymic Bipolar Patients During an Emotional Go/NoGo Task. *American Journal of Psychiatry*, *164*(4), 638–646. https://doi.org/10.1176/ajp.2007.164.4.638

Westlye, L. T., Walhovd, K. B., Dale, A. M., Bjørnerud, A., Due-Tønnessen, P., Engvig, A., Grydeland, H., Tamnes, C. K., Østby, Y., & Fjell, A. M. (2010). Life-Span Changes of the Human Brain White Matter: Diffusion Tensor Imaging (DTI) and Volumetry. *Cerebral Cortex*, *20*(9), 2055–2068. https://doi.org/10.1093/cercor/bhp280

White, T., Gilleen, J., & Shergill, S. (2013). Dysregulated but not decreased salience network activity in schizophrenia. *Frontiers in Human Neuroscience*, *7*. https://www.frontiersin.org/articles/10.3389/fnhum.2013.00065

Winterer, G., Konrad, A., Vucurevic, G., Musso, F., Stoeter, P., & Dahmen, N. (2008). Association of 5′ end neuregulin-1 (NRG1) gene variation with subcortical medial frontal microstructure in humans. *NeuroImage*, *40*(2), 712–718. https://doi.org/10.1016/j.neuroimage.2007.12.041

Wise, T., Radua, J., Via, E., Cardoner, N., Abe, O., Adams, T. M., Amico, F., Cheng, Y., Cole, J. H., de Azevedo Marques Périco, C., Dickstein, D. P., Farrow, T. F. D., Frodl, T., Wagner, G., Gotlib, I. H., Gruber, O., Ham, B. J., Job, D. E., Kempton, M. J., … Arnone, D. (2017). Common and distinct patterns of grey-matter volume alteration in major depression and bipolar disorder: Evidence from voxel-based meta-analysis. *Molecular Psychiatry*, *22*(10), Article 10. https://doi.org/10.1038/mp.2016.72

Wright, P. J., Mougin, O. E., Totman, J. J., Peters, A. M., Brookes, M. J., Coxon, R., Morris, P. E., Clemence, M., Francis, S. T., Bowtell, R. W., & Gowland, P. A. (2008). Water proton T1 measurements in brain tissue at 7, 3, and 1.5T using IR-EPI, IR-TSE, and MPRAGE: Results and optimization. *Magnetic Resonance Materials in Physics, Biology and Medicine*, *21*(1), 121. https://doi.org/10.1007/s10334-008-0104-8

Yarnykh, V. L. (2010). Optimal radiofrequency and gradient spoiling for improved accuracy of T1 and B1 measurements using fast steady-state techniques. *Magnetic Resonance in Medicine*, *63*(6), 1610–1626. https://doi.org/10.1002/mrm.22394

Young, R. C., Biggs, J. T., Ziegler, V. E., & Meyer, D. A. (1978). A rating scale for mania: Reliability, validity and sensitivity. *The British Journal of Psychiatry*, *133*(5), 429–435.

Zatorre, R. J., Fields, R. D., & Johansen-Berg, H. (2012). Plasticity in gray and white: Neuroimaging changes in brain structure during learning. *Nature Neuroscience*, *15*(4), Article 4. https://doi.org/10.1038/nn.3045

Zhang, W., Cai, S., Huang, K., Lv, Y., Kang, Y., Wang, Q., & Huang, L. (2019). Association between schizophrenia risk allele dosage of rs6994992 and whole-brain structural and functional characteristics. *Psychiatry Research: Neuroimaging*, *294*, 110956. https://doi.org/10.1016/j.pscychresns.2019.05.005